Molecular Therapy
Methods & Clinical Development
Original Article

Superior Expansion and Cytotoxicity of Human Primary NK and CAR-NK Cells from Various Sources via Enriched Metabolic Pathways

Yan Yang,[1,3] Saiaditya Badeti,[1,3] Hsiang-chi Tseng,[1] Minh Tuyet Ma,[1] Ting Liu,[1] Jie-Gen Jiang,[1] Chen Liu,[1] and Dongfang Liu[1,2]

[1]Department of Pathology, Immunology and Laboratory Medicine, Rutgers New Jersey Medical School, 185 South Orange Avenue, Newark, NJ 07103, USA; [2]Center for Immunity and Inflammation, New Jersey Medical School, Rutgers-The State University of New Jersey, 205 South Orange Avenue, Newark, NJ 07101, USA

Clinical success of chimeric antigen receptor (CAR) T cell immunotherapy requires the engineering of autologous T cells, which limits the broader implementation of CAR cell therapy. The development of allogeneic and universal cell products will significantly broaden their application and reduce costs. Allogeneic natural killer (NK) cells can be used for universal CAR immunotherapy. Here, we develop an alternative approach for the rapid expansion of primary NK and CAR-NK cells with superior expansion capability and *in vivo* cytotoxicity from various sources (including peripheral blood, cord blood, and tumor tissue). We apply a human B-lymphoblastoid cell-line 721.221 (hereinafter, 221)-based artificial feeder cell system with membrane-bound interleukin 21 (mIL-21) to propagate NK and CAR-NK cells. The expansion capability, purity, and cytotoxicity of NK cells expanded with 221-mIL-21 feeder cells are superior to that of conventional K562-mIL-21 feeder cells. RNA sequencing (RNA-seq) data show that 221-mIL-21 feeder cell-expanded NK cells display a less differentiated, non-exhausted, limited fratricidal, memory-like phenotype correlated with enriched metabolic pathways, which explains underlying mechanisms. Thus, "off-the-shelf" NK and CAR-NK cells with superior functionalities and expansion using a genetically modified 221-mIL-21 feeder cell expansion system will greatly support clinical use of NK immunotherapy.

INTRODUCTION

Natural killer (NK) cells are an important subset of lymphocytes for providing our body's first line of defense.[1] NK cells were originally described for their capacity to spontaneously kill tumor cells without prior sensitization,[2–6] which distinguishes them from cytotoxic T lymphocytes (CTLs). NK cells kill tumor cells or virally infected cells via several pathways,[1,7,8] which include direct cytotoxicity (natural cytotoxicity and antibody-dependent cell-mediated cytotoxicity [ADCC]) and through indirect effects (e.g., cytokine production and interacting with adaptive immunity).[1] An important application of NK cells is the use of primary *ex vivo*, expanded NK cells or genetically modified NK cells to treat various cancers because of their less severe adverse effects.[9,10] Several clinical trials have shown that NK or chimeric antigen receptor (CAR)-NK cell infusion is associated with a milder graft-versus-host disease (GvHD) compared to T cell infusion.[9,10] There are two major clinical applications of NK cells. The first one is to use primary *ex vivo* expanded NK cells without any genetic modification to treat cancers. Specifically, NK cells are currently used to treat acute myelocytic leukemia (AML) and acute lymphocytic leukemia (ALL) clinically.[11–13] The second application is to use genetically modified NK cells expanded *in vitro* to treat patients. Genetically modified NK cells, such as –CAR-modified NK cells, have become an emerging tool for cancer immunotherapy.[14,15] Clinical investigation on the use of CAR-modified NK cell-based immunotherapy has been extensively conducted against a wide variety of cancers.[16] Similar to CAR-T cell-based immunotherapy, genetically modified NK cells using various CAR molecules to redirect antigen specificity has been investigated by different groups.[16–18]

CAR-modified T cell therapy has become a promising immunotherapeutic strategy for the treatment of several cancers,[19–21] and it has gained a significant amount of attention from researchers both in academia and in industry.[18] Adoptive transfer of these CAR-modified T cells into patients has shown remarkable success in treating multiple types of blood cancers, such as refractory acute lymphoblastic leukemia.[22–24] Additionally, clinical trials treating multiple myeloma,[25,26] leukemia,[19,22–24] sarcoma,[27] and neuroblastoma[28,29] using CAR products have reported promising patient outcomes. Considerable efforts and funds are being invested into CAR development and optimization.[30–33]

Current adoptive CAR-T cell therapy combines tumor antigen specificity with immune cell activation in a single receptor. The process involves isolating a patient's own T cells, engineering them to express

Received 2 June 2020; accepted 18 June 2020;
https://doi.org/10.1016/j.omtm.2020.06.014.

[3]These authors contributed equally to this work.

Correspondence: Dongfang Liu, PhD, Department of Pathology, Immunology and Laboratory Medicine, Rutgers New Jersey Medical School, 185 South Orange Avenue, Newark, NJ 07103, USA.
E-mail: dongfang.liu@rutgers.edu

CARs that recognize tumor proteins, and re-infusing them back into the patient. One of the problems with current adoptive CAR-T cell therapies is the use of autologous T cells isolated from patients. Autologous T cells have several major issues: (1) T cells directly isolated from immune-compromised cancer patients usually have poor cytotoxicity and functionality, precluding their use; (2) autologous T cells cannot be used for other patients due to the potential risk of developing severe GvHD; and (3) CAR-T cell therapy is associated with significant side effects, such as cytokine release syndrome (CRS) and other side effects.[34–38] Given these risks and the high cost of immunotherapy,[39] it is becoming imperative to develop an alternative, "off-the-shelf" cell type for immunotherapy.

To alleviate these disadvantages of CAR-T cell immunotherapy, additional cytotoxic-cell-mediated immunotherapies are urgently needed. The unique biology of NK or CAR-NK cells may allow them to serve as a safer, effective, alternative immunotherapeutic strategy to CAR-T cells in the clinic.[9] Here, we developed an alternative method to expand human primary NK cells directly from PBMCs (peripheral blood mononuclear cells) and CB (cord blood), as well as tumor tissue, using an irradiated, genetically engineered 721.221 (hereinafter, 221) cell line (a B cell line derived through mutagenesis that does not express dominant major histocompatibility complex [MHC] class I molecules or expresses a low amount of MHC class I molecules)[40] that expresses membrane-bound interleukin 21 (IL-21) (221-mIL-21), as previous studies show the importance of IL-21 in NK expansion.[41–45] In combination with two recombinant cytokines (IL-15 and IL-2), primary NK cells were expanded nearly 100,000-fold after 2 to 3 weeks of expansion. Furthermore, transduction with retrovirus coding for a CAR molecule specific for CD19 protein resulted in the expansion of primary NK cells from both PBMCs and CB. We also investigated the potential molecular mechanisms by immunophenotyping and RNA sequencing (RNA-seq) of both NK and feeder cells. The 221-mIL-21 feeder-cell-expanded NK cells display a less differentiated, non-exhausted, limited fratricidal, memory-like phenotype correlated with enriched metabolic pathways. In summary, we generated an alternative platform for the expansion of human primary NK cells and genetically modified CAR-NK cells via enriched metabolic pathways, which can lead to the development of feasible, "off-the-shelf" clinical-grade CAR-NK products in the near future.

RESULTS

Generation of Membrane Form of IL-21 on Artificial Antigen-Presenting Cell Lines

Previous studies have shown that IL-21 plays a critical role in NK cell proliferation and promotes the expansion of memory-like NK cells.[41–43] Moreover, clinical trials showed that NK cells and CAR-NK cells expanded with K562 expressing mIL-21 can be safely infused.[10,44] Here, we developed an artificial antigen-presenting cell line using the 221 cell line expressing a membrane form of IL-21 without noticeable phenotype changes (Figure S1). Additionally, we also examined the expression of the IL-21 receptor on human primary NK cells (Figure S2).

To set up a human primary NK cell expansion system, IL-21 was cloned into an SFG retroviral vector that contains a human immunoglobulin G1 (IgG1) hinge and CH2-CH3 domain, CD28 transmembrane (TM) domain and intracellular domain, 4-1BB (4-1BB) intracellular domain, and CD3zeta intracellular domain (Figure 1A). In this study, the SFG retroviral vector (containing the IgG1 CH2-CH3 domain, CD28 TM and intracellular domains, 4-1BBL intracellular domain, and CD3zeta intracellular domain) was used to ensure high transduction efficiency and stable cell-surface protein expression. As a control, wild-type (WT) K562 (a human myelogenous leukemia cell line),[46] K562-mIL-21, and WT 221 were included in the assays. K562 and 221 cells were transduced with IL-21 retrovirus and sorted using fluorescence-activated cell sorting (FACS) by staining with anti-human IL-21 antibody. After 2 weeks of culture, the expression levels of mIL-21 on K562-mIL-21 and 221-mIL-21 were further verified using flow cytometry. High levels of mIL-21 were expressed on both K562-mIL-21 cells (Figure S1A) and 221-mIL-21 cells (Figure S1B). Both K562-mIL-21 and 221-mIL-21 cells were also stained with anti-IL-21 antibody and evaluated for proper plasma membrane localization of the IL-21 protein by confocal microscopy (Figures S1C and S1D). RNA-seq data also suggested changes of gene expression profile between transduced and non-transduced cells (Figure S3). RNA-seq data also demonstrated different expression patterns of ligands for NK-activating receptors and MHC class I/II molecules between 221 and K562 feeder cells, as well as between K562-mIL-21 and 221-mIL-21 feeder cells (Figure S3). As co-stimulatory molecules 4-1BBL (also known as CD137L and TNFSF9) and OX40L (also known as CD252 and TNFSF4, a ligand for OX40 [also known as CD134 or TNFRSF4]) play important roles in NK cell proliferation,[45,47] the 4-1BBL and OX40L RNA expression levels among these feeder cells were analyzed (Figure S3E), and it was revealed that 221-mIL-21 feeder cells express slightly higher levels of 4-1BBL and OX40L than K562-mIL-21 feeder cells.

Next, we determined whether the transduction of mIL-21 molecules onto the cell surface of K562 and 221 feeder cells can alter the expression of major activating and inhibitory ligands of NK cells. 4-1BBL (a ligand of 4-1BB), ICAM-1 (a ligand of LFA-1), PD-L1 (a ligand of PD-1), HLA-E (human leukocyte antigen-E; a ligand for CD94/NKG2A or CD94/NKG2C), and MICA/B (a ligand of NKG2D) were examined by flow cytometry. Their expressions were comparable at pre- and post-transduction stages (Figures S1E, S1G, and S1H). In summary, we have successfully established the stable membrane expression of IL-21 in both K562 and 221 cells for NK expansion.

Superior Propagation of NK Cells by 221-mIL-21 Cells among Different Types of Feeder Cells

After establishment of K562, K562-mIL-21, 221, and 221-mIL-21 cell lines as feeder cells, the next task was to determine which feeder cell line can optimally expand human primary NK or CAR-NK cells. To expand human primary NK cells from peripheral blood (hereinafter, PBNK cells), PBMCs were isolated from buffy coats from healthy donors and co-cultured with feeder cells, 200 U/mL IL-2, and 5 ng/mL

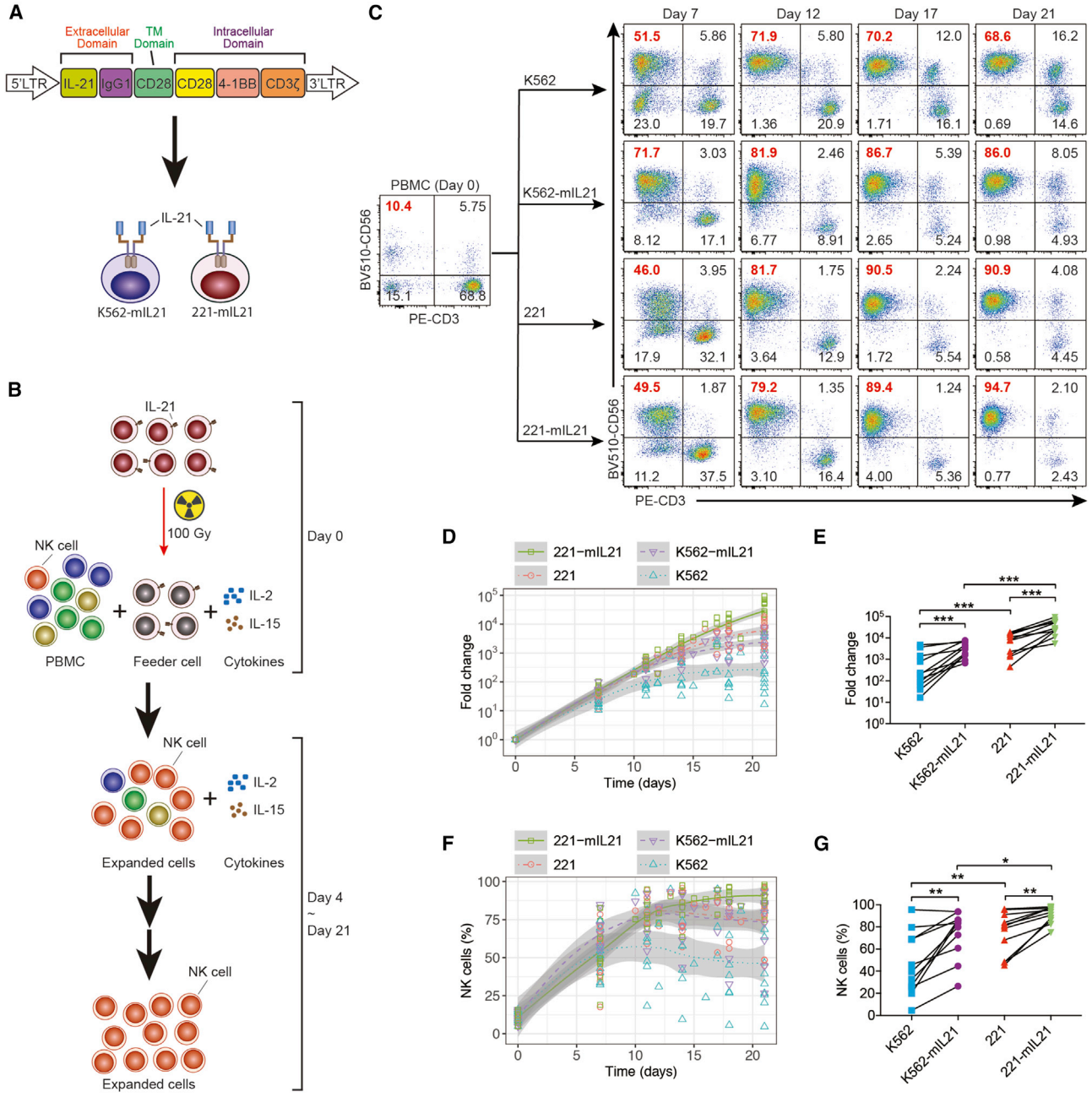

Figure 1. Superior Propagation of Human PBNK Cells by 221-mIL-21 Cells among Different Types of Feeder Cells

(A) Schematic representation of recombinant retroviral vector encoding the extracellular domain of human IL-21. (B) Schematic representation of primary human NK cell expansion with membrane expressing IL-21 feeder cells. Feeder cells were irradiated with a dose of 100 Gy (10,000 rad), and then PBMCs were co-cultured with irradiated feeder cells with IL-2 and IL-15 for NK cell expansion. (C) Representative flow cytometry plots of the purity of NK cells expanded with different feeder cell systems at indicated days post-expansion. PBMCs were stimulated with irradiated K562, K562-mIL-21, 221, and 221-mIL-21 cells on day 0. The purities of NK cells were determined at the indicated time points. (D) Dynamic time-lapsed expansion data of the fold expansion of NK cells from 11 donors expanded with irradiated K562, K562-mIL-21, 221, and 221-mIL-21 feeder cells for the indicated time points. (E) Quantitative data of the fold expansion of NK cells from 11 donors expanded with irradiated feeder cells on day 21. (F) Dynamic time-lapsed expansion data of the purities of NK cells from 11 donors expanded with irradiated K562, K562-mIL-21, 221, and 221-mIL-21 feeder cells for 21 days. (G) Quantitative data of the purities of NK cells from 11 donors expanded with irradiated feeder cells on day 21. Means (solid lines) with 95% confidence interval (CI) (gray band) are indicated in (D) and (F). *$p < 0.05$; **$p < 0.01$; ***$p < 0.001$. Error bars represent the Standard Error of the Mean (SEM).

IL-15. To compare their relative ability to stimulate NK cell expansion, both K562-mIL-21 and 221-mIL-21 cells were compared directly. WT-K562 and WT-221 cell lines (hereinafter referred to as K562 and 221, respectively) were used as control groups (Figure 1B). The initial number of PBMCs and proportion of NK cells were 5 million and 10%–20%, respectively. Representative NK expansion profiles for each cell line at different time points (days 0, 7, 12, 17, and 21) gated on CD3 and CD56 by flow cytometry were shown (Figure 1C). The dynamic fold changes and the proportion of NK cells were significantly increased after 3 weeks of expansion by co-culturing PBMCs with different feeder cells (Figures 1D–1G). As expected, feeder cells expressing mIL-21 showed significantly higher efficiency of expansion and higher purity of NK cells compared to the corresponding WT feeder cells (221-mIL-21 versus 221 and K562-mIL-21 versus K562). Moreover, the fold increase after expansion of NK cells with 221-mIL-21 feeder cells and the relative purity of expanded NK cells was significantly higher than that of K562-mIL-21 feeder cells. Interestingly, WT-221 feeder cells also showed a better NK cell expansion compared to WT-K562 feeder cells (Figures 1D–1G). Additionally, the non-NK cell populations (including $CD3^+CD56^-$, $CD3^+CD56^+$, and $CD3^-CD56^-$ cells) are decreased in the presence of mIL-21-expressing feeder cells (Figure S4).

To explore the potential mechanisms underlying superior expansion capability exerted by 221-mIL-21 feeder cells, we compared the proliferation and apoptosis of NK cells. NK cells expanded by 221-mIL-21 feeder cells showed better proliferation and less apoptosis, compared to NK cells expanded by K562-mIL-21 feeder cells (Figure S5). In summary, 221-mIL-21 cells are superior to K562-mIL-21 cells as feeder cells for expanding human primary NK cells, which can be explained by superior proliferation and less apoptosis during expansion.

Characteristics of Expanded PBNK Cells and NK Cells Derived from CB

To determine the immunophenotyping of K562, K562-mIL-21, 221, and 221-mIL-21 expanded PBNK cells, we used flow cytometry to characterize several important activating and inhibitory receptors. The activating receptors include CD16, NKG2D, NKp46, 2B4, DNAM-1, CD94, CD8a, and NKG2C (Figures 2A and 2B). The inhibitory receptors include NKG2A, CTLA-4, KLRG1, PD-1, LIR1, TIM-3, TIGIT, LAG-3, total KIR, KIR2DL1, KIR2DL2/L3, KIR3DL1, and KIR3DL2 (Figures 2C–2E). The expression of these activating and inhibitory receptors on expanded NK cells is comparable. Interestingly, CD69, an activation marker of NK cells, was increased in the K562-mIL-21-expanded NK cells compared to 221-mIL-21-expanded NK cells.

To determine whether these *ex vivo* expanded PBNK cells exhibit similar functions, we examined the cytotoxicity of expanded PBNK cells by co-culturing them with the NK susceptible 221 and K562 target cells (Figure S6). Interestingly, NK cells expanded with 221-mIL-21 cells show superior cytotoxicity, compared to NK cells expanded with K562-mIL-21 cells (Figure S6). To further confirm this observation, we used the CD107a assay to determine the surface level of CD107a molecules after NK degranulation. A slightly higher percentage of degranulated NK cells expanded with K562-mIL-21 was observed, compared to that with 221-mIL-21 expanded NK cells (Figure S7), indicating possible unpolarized, spontaneous degranulation on K562-mIL-21 expanded NK cells.

Recently, CB-derived CD19-CAR-NK cells were successfully used to treat non-Hodgkin's lymphoma (NHL) or chronic lymphocytic leukemia (CLL).[10] To further examine whether NK cells isolated from CB (CBNK cells) can be expanded by this system, we compared the expansion of CBNK cell number and purity between K562-mIL-21 and 221-mIL-21 feeder cells. The number of CBNK cells expanded with 221-mIL-21 feeder cells was significantly higher than that of K562-mIL-21 feeder cells (Figure S8). The purity of CBNK cells and other types of cells (including $CD3^+CD56^-$, $CD3^+CD56^+$, and $CD3^-CD56^-$ cells) was comparable between K562-mIL-21 and 221-mIL-21 feeder cells (Figure S8). Comparable cytotoxicity between 221-mIL-21 expanded CBNK and K562-mIL-21 expanded CBNK cells was observed (Figure S9). When comparing the killing activity between PBNK and CBNK cells (Figures S6C and S9), the CBNK killing toward K562 seemed to be greater than that of PBNK, which suggests that CB would be a more optimal source than peripheral blood.

We further examined the immunophenotyping of expanded NK cells by K562-mIL-21 and 221-mIL-21 expanded CBNK cells using flow cytometry (Figures 2F–2H). Interestingly, CD69 expression is dramatically decreased in 221-mIL-21 expanded CBNK cells, with comparable cytotoxicity between 221-mIL-21 expanded CBNK and K562-mIL-21 expanded CBNK cells (Figures 2G and S9).

In summary, expanded 221-mIL-21 expanded CBNK cells show surface receptors similar to those of 221-mIL-21 expanded PBNK cells. Decreased CD69 surface expression on both CBNK and PBNK cells suggests that 221-mIL-21 expanded NK cells exhibit a less activated status.

Improved Peripheral-Blood-Derived CAR-NK Expansion Using 221-mIL-21 Cells

CAR-NK immunotherapy has become a promising strategy for cancer treatments.[9] We further determined whether 221-mIL-21 feeder cells could similarly expand CAR-modified NK cells. The SFG retroviral vector containing an anti-CD19 scFv, a human IgG1 hinge and CH2-CH3 domain, CD28 TM domain and intracellular domain, 4-1BB intracellular domain, and CD3zeta intracellular domain was used (Figure 3A). To expand CAR-NK cells *ex vivo*, unfractionated PBMCs were stimulated for 7 days with 221-mIL-21 feeder cells in the presence of soluble IL-2 and IL-15, inducing rapid proliferation of NK cells and, in some cases, non-specific expansion of T cells. At day 7, expanded NK cells were transduced with CD19-CAR retrovirus (Figure 3B). Please note that unfractionated PBMCs were used to expand CAR-NK cells in this study. NK cell number and

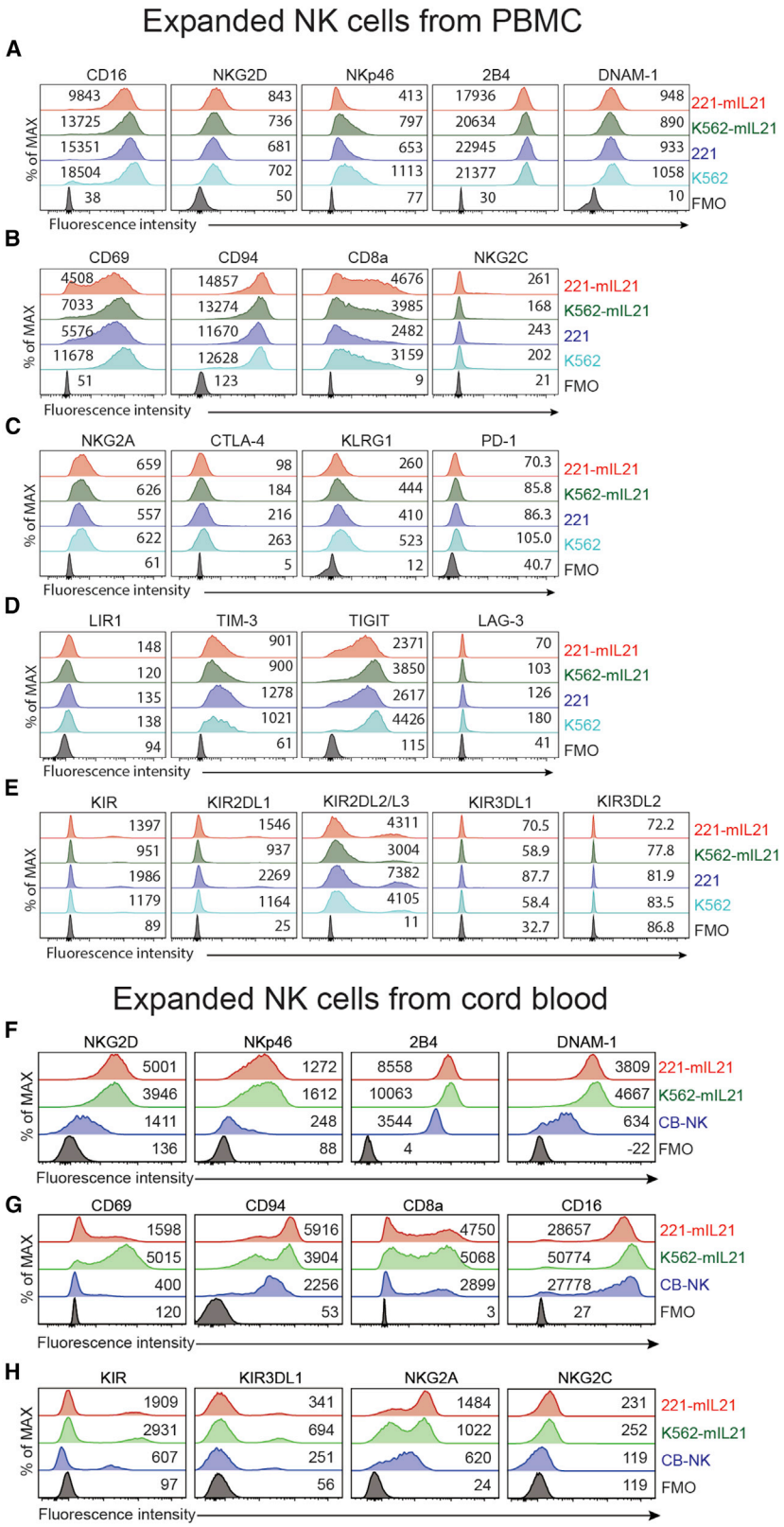

Figure 2. Phenotypes of NK Cells Expanded by Different Feeder Cells

(A) Representative histograms of the expression of CD16, NKG2D, NKp46, 2B4, and DNAM-1 on NK cells expanded from PBMCs using K562, K562-mIL-21, 221, and 221-mIL-21 feeder cells. The mean fluorescence intensity (MFI) is noted in the respective histograms. (B) Representative histograms of the expression of CD69, CD94, CD8a, and NKG2C on PBNK cells expanded using K562, K562-mIL-21, 221, and 221-mIL-21 feeder cells, respectively. The MFI is noted in the respective histograms. (C) Representative histograms of the expression of NKG2A, CTLA-4, KLRG1, and PD-1 on PBNK cells expanded using K562, K562-mIL-21, 221, and 221-mIL-21 feeder cells, respectively. The MFI is noted in the respective histograms. (D) Representative histograms of the expression of LIR1, TIM-3, TIGIT, and LAG-3 on PBNK cells expanded using K562, K562-mIL-21, 221, and 221-mIL-21 feeder cells, respectively. The MFI is noted in the respective histograms. (E) Representative histograms of the expression of KIR, KIR2DL1, KIR2DL2/L3, KIR3DL1, and KIR3DL2 on PBNK cells expanded using K562, K562-mIL-21, 221, and 221-mIL-21 feeder cells. The MFI is noted in the respective histograms. (F) Representative histograms of the expression of NKG2D, NKp46, 2B4, and CD226 on NK cells expanded from CB mononuclear cells using 221-mIL-21 (red) and K562-mIL-21 (green) feeder cells. NK cells from freshly isolated CB mononuclear cells from the same donor are also indicated (blue). (G) Representative histograms of the expression of CD69, CD94, CD8a, and CD16 on NK cells expanded from CB mononuclear cells using 221-mIL-21 (red) and K562-mIL-21 (green) feeder cells. NK cells from freshly isolated CB mononuclear cells from the same donor are also indicated (blue). (H) Representative histograms of the expression of NKG2A, NKG2C, KIR, and KIR3DL1 on NK cells expanded from CB mononuclear cells using 221-mIL-21 (red) and K562-mIL-21 (green) feeder cells. NK cells from freshly isolated CB mononuclear cells from the same donor are also indicated (blue).

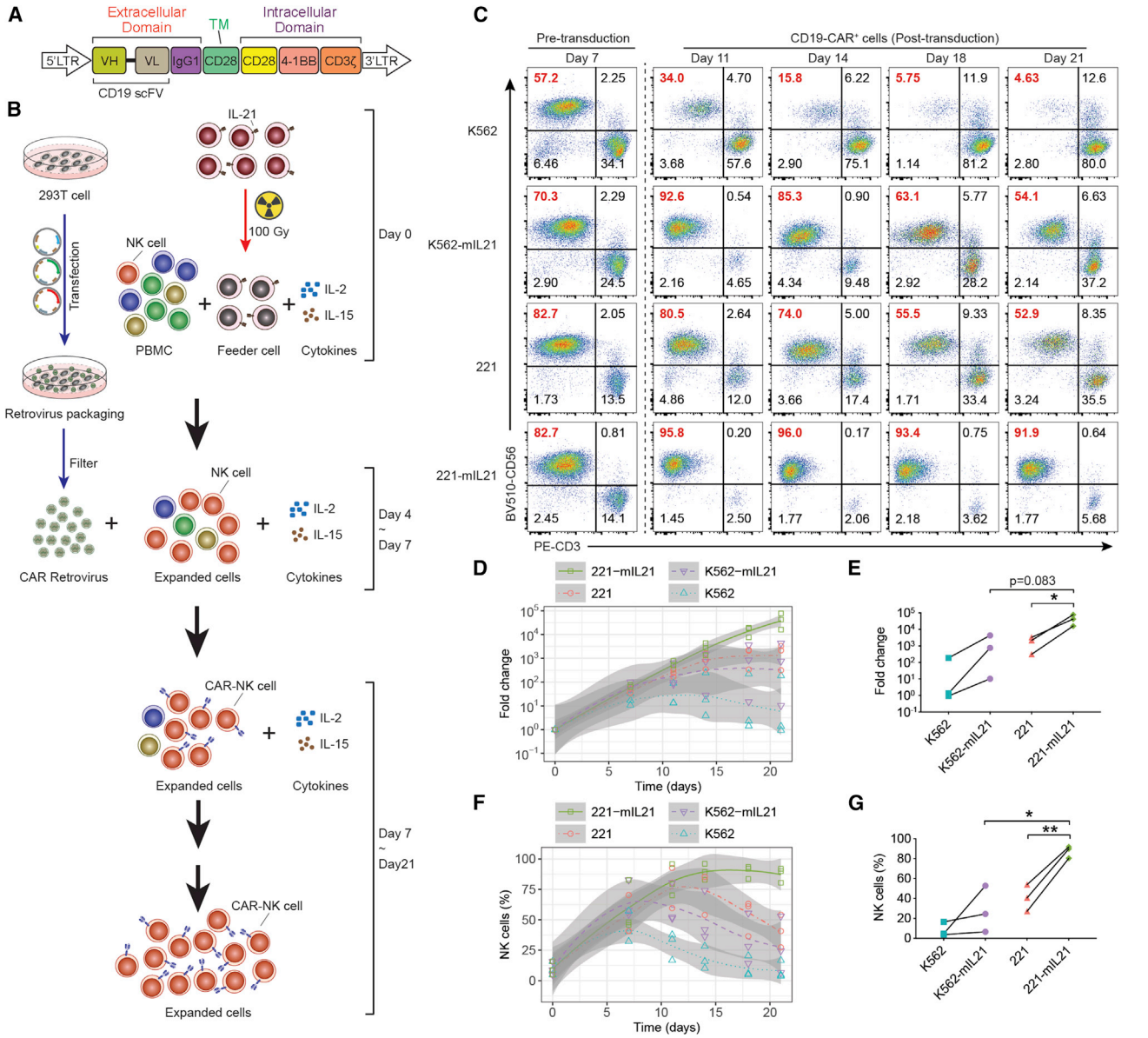

Figure 3. Improved Expansion Capability of Peripheral-Blood-Derived CAR-NK Cells Using the 221-mIL-21 Feeder Cell System

(A) Schematic representation of retroviral vector encoding the CD19-CAR design. (B) Schematic experimental design of CD19-CAR-modified NK cell expansion with the 221-mIL-21 feeder cell system. 221-mIL-21 cells were irradiated with a dose of 100 Gy (10,000 rad). Then, PBMCs were co-cultured with irradiated feeder cells in the presence of IL-2 and IL-15. In parallel, CD19-CAR retrovirus was produced by transfecting 293T cells. The expanded NK cells were transduced with CD19-CAR retrovirus at day 7. Cells were cultured for 21 days. (C) Representative flow cytometry dot plots of the percentage of expanded CD19-CAR-positive expanded NK cells at indicated days post-expansion. PBMCs were stimulated with irradiated 221-mIL-21 on day 0 and transduced with CD19-CAR retrovirus on day 7. The purity of NK cells within CD19-CAR-positive cells was checked every 3 to 4 days. (D) Dynamic time-lapsed expansion data of the fold expansion of CD19-CAR-NK cells from 3 donors. CD19-CAR-modifed NK cells were expanded with irradiated K562, K562-mIL-21, 221, and 221-mIL-21 feeder cells for 21 days. (E) Quantitative data of the fold expansion of CD19-CAR-NK cells from 3 donors on day 21 of expansion. (F) Dynamic time-lapsed expansion data of the purity of NK cells within CD19-CAR-positive cells from 3 donors. NK cells were expanded with irradiated K562, K562-mIL-21, 221, and 221-mIL-21 feeder cells. (G) Quantitative data of the percentage of NK cells within CD19-CAR-positive cells from 3 donors on day 21 post-expansion. Means (solid lines) with 95% CI (gray band) are indicated in (D) and (F). *p < 0.05; **p < 0.01. Error bars represent SEM.

purity were examined at day 7, day 11, day 14, day 18, and day 21. A representative profile of *ex vivo* expanded NK cells from a single donor shows superior NK number and purity (Figure 3C). The quantitative analysis of NK cell number (Figures 3D and 3E) and purity (Figures 3F and 3G) from 3 donors shows that 221-mIL-21 feeder cells provide superior CD19-CAR-NK cell expansion.

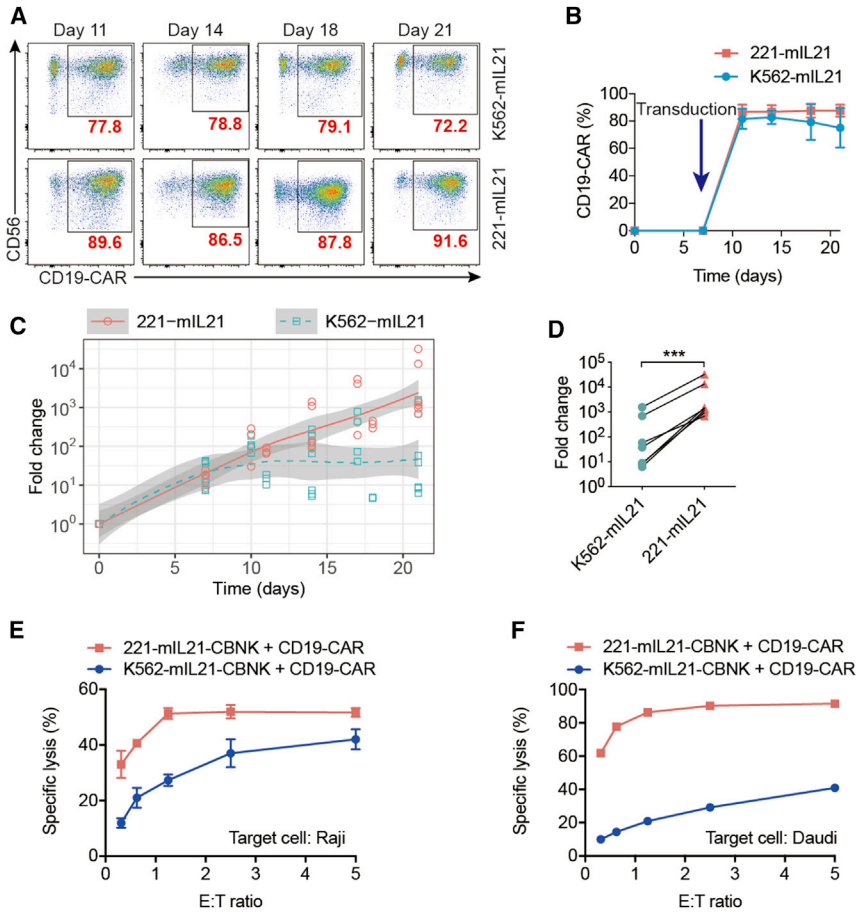

Figure 4. Superior Cytotoxicity of CB-Derived CD19-CAR-NK Cells Using 221-mIL-21 Feeder Cells

(A) Representative flow cytometry dot plots of the percentage of CD19-CAR-positive cells in NK cells at the indicated days. CBMCs were stimulated with irradiated feeder cells on day 0 and transduced with CD19-CAR retrovirus on day 7. (B) Quantitative data of the percentage of CD19-CAR-positive cells in NK cells expanded from CBMCs (n = 6). (C) Dynamic time-lapsed expansion data of the fold expansion of CD19-CAR-CBNK cells from 6 donors. CD19-CAR-modifed NK cells were expanded with irradiated K562-mIL-21 and 221-mIL-21 feeder cells for 21 days. (D) Quantitative data of the fold expansion of CD19-CAR-CBNK cells from 6 donors on day 21 of expansion. (E) Quantitative data of the cytotoxic activity of expanded CD19-CAR-CBNK cells against Raji cells using the CFSE/7-AAD cytotoxicity assay. Target cells were labeled with CFSE and then incubated with expanded CD19-CAR-CBNK cells at E:T ratios ranging from 5:1 to 0.3125:1 for 4 h. Then, 7-AAD was used to determine the lysis of target cells. (F) Quantitative data of the cytotoxic activity of expanded CD19-CAR-CBNK cells against Daudi cells using the CFSE/7-AAD cytotoxicity assay. ***p < 0.001. Error bars represent SEM.

The percentage of CD19-CAR-positive NK cells stimulated by K562-mIL-21 was comparable to that of CD19-CAR-NK cells stimulated by 221-mIL-21 cells (Figure S10). In contrast, non-NK cells (including $CD3^+CD56^-$, $CD3^+CD56^+$, and $CD3^-CD56^-$ populations) are decreased in the presence of mIL-21-expressing feeder cells (Figure S10). In conclusion, 221-mIL-21 feeder cells show a superior CAR-NK cell expansion capability compared to that of K562-mIL-21 feeder cells.

221-mIL-21 Feeder Cells Exhibit Superior Capability to Expand Cord-Blood-Derived Primary NK and CD19-CAR-CBNK Expansion

Given the reported advantages of CBNK and CAR-NK cells,[14,48,49] we further tested whether the 221-mIL-21 feeder expansion system could also expand CB-derived CAR-NK cells. To expand CBNK cells *ex vivo*, unfractionated CB lymphocytes were stimulated for 7 days with 221-mIL-21 feeder cells in the presence of soluble IL-2 and IL-15, inducing rapid proliferation of CBNK cells (Figure 4). As a control, unfractionated CB lymphocytes were stimulated with K562-mIL-21 feeder cells in the presence of soluble IL-2 and IL-15 in a separate group. At day 7, expanded CBNK cells were transduced with CD19-CAR retrovirus. A representative profile of *ex vivo* expanded CBNK cells from one donor shows the superior purity of CD19-CAR-CBNK cells (Figure 4A). The quantitative analysis of CD19-CAR-CBNK cell purity, measured by the percentage of CD19-CAR-positive CBNK cells from 3 donors shows that 221-mIL-21 feeder cells provide a slightly superior CD19-CAR-CBNK cell purity (Figure 4B). The quantitative analysis of CD19-CAR-CBNK cell number from 6 donors also demonstrates that 221-mIL-21 feeder cells provide a superior CD19-CAR-CBNK cell number (Figures 4C and 4D).

To determine whether these *ex vivo* expanded CD19-CAR-CBNK cells exhibit similar functions, we examined expanded CD19-CAR-CBNK cell (at 21-day expansion) cytotoxicity by co-culturing them with the CD19-positive Raji and Daudi cells. Interestingly, CD19-CAR-CBNK cells expanded with 221-mIL-21 feeder cells show superior cytotoxicity, compared with CD19-CAR-CBNK cells expanded with K562-mIL-21 cells (Figures 4E and 4F). Therefore, we successfully developed an NK expansion approach with improved CBNK and CAR-NK expansions using 221-mIL-21 feeder cells.

Effectiveness and Side Effects of Expanded CAR-NK Cells *In Vivo*

To further evaluate whether the expanded CD19-CAR-NK cells can kill tumor cells *in vivo*, we compared the anti-tumor activities between 221-mIL-21 expanded CD19-CAR-NK cells and K562-mIL-21 expanded CD19-CAR-NK cells using lymphoma xenograft models in NOD.Cg-*Prkdc*^{scid} *Il2rg*^{tm1Wjl}/SzJ (NSG) mice (Figure 5). Briefly, luciferase-tagged Raji (FFluc-Raji) were implanted by intravenous tail vein injection. Mice were infused with CD19-CAR-NK cells

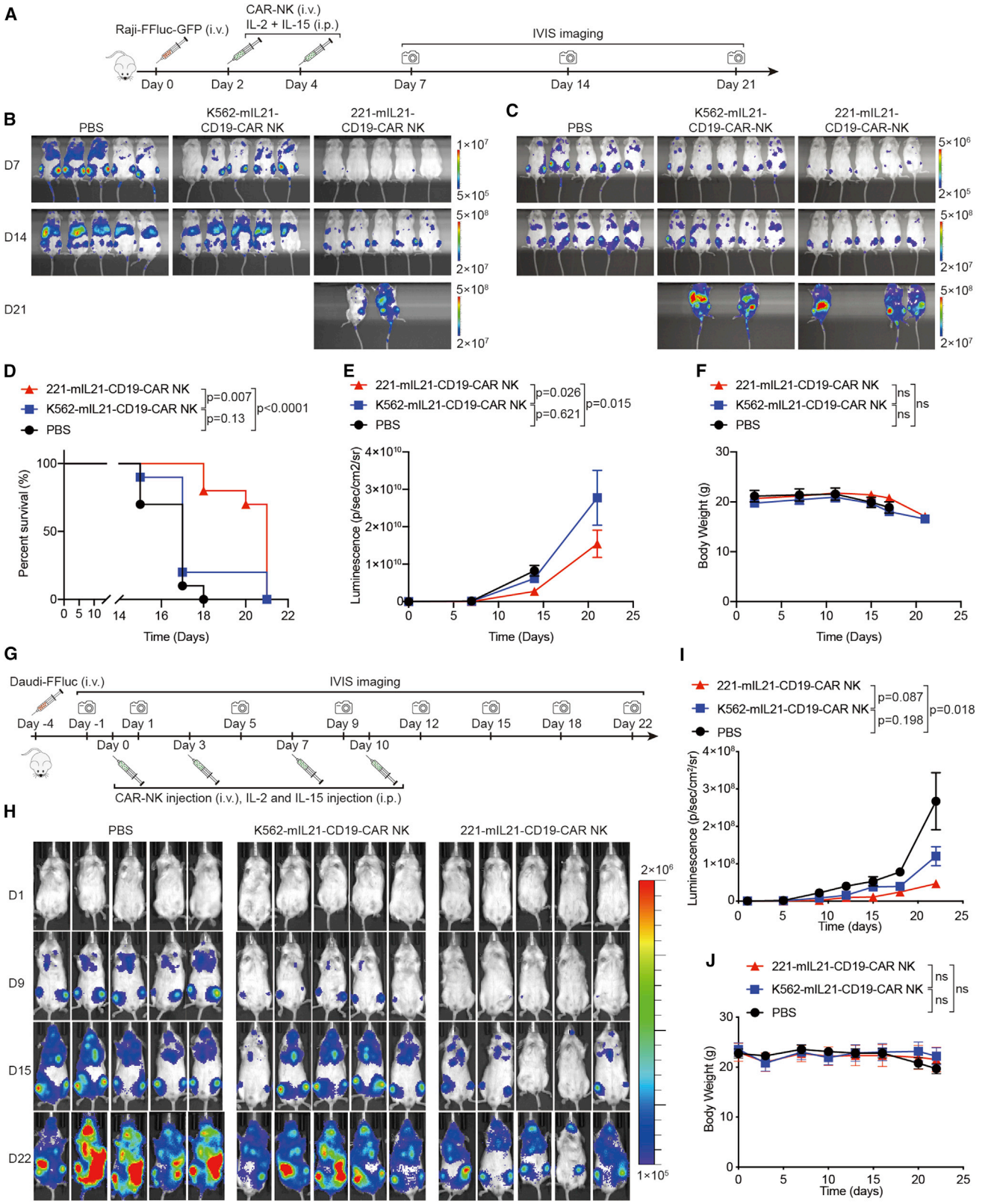

(legend on next page)

expanded from peripheral blood with different feeder cells. Tumor burden was evaluated at indicated time points by measuring tumor-derived bioluminescence (Figure 5A). A superior anti-tumor response was observed in mice treated with 221-mIL-21 expanded CD19-CAR-NK cells compared to those that were treated with K562-mIL-21 expanded CD19-CAR-NK cells (Figure 5B–5E). To further evaluate the toxicity of these *in vivo* expanded CD19-CAR-NK cells, we quantified the body weight of mice. No significant difference in body weights was observed (Figure 5F), indicating minimal side effects of CD19-CAR-NK cells.

To further compare the efficacy of CD19-CAR-NK cells between 221-mIL-21 and K562-mIL-21 feeder cells, we used another CD19-positive Daudi cell line to establish a lymphoma xenograft model in NSG mice. Briefly, luciferase-tagged Daudi (FFluc-Daudi) were implanted by intravenous tail vein injection. Tumor burden was assessed at indicated time points by measuring tumor-derived bioluminescence following CD19-CAR-NK infusion therapy (Figure 5G). As expected, mice treated with 221-mIL-21 expanded CD19-CAR-NK cells showed superior anti-tumor activities compared with those treated with K562-mIL-21 expanded CD19-CAR-NK cells (Figures 5H and 5I). Similar results on tumor growth inhibition (TGI) were obtained (data not shown). To further evaluate the toxicity of these *in vivo*-expanded CD19-CAR-NK cells, we quantified the body weight of mice. No significant difference in body weights was observed (Figure 5J). In conclusion, 221-mIL-21-expanded CD19-CAR-NK cells show superior anti-tumor activities *in vivo* with minimal adverse effects.

221-mIL-21 Feeder Cell Expansion System Promotes a Less Differentiated, Memory-like NK Cell Development with Enriched Metabolic Pathways

To explain why the 221-mIL-21 feeder cell expansion system induces superior NK cell expansion capability and functions, we performed RNA-seq experiments using NK cells expanded by different feeder cell systems and at various time points. Briefly, PBMCs were stimulated with irradiated K562-mIL-21 or 221-mIL-21 feeder cells. Expanded NK cells from these two different expansion systems were sorted using flow cytometry on day 7 and day 14 for RNA-seq analysis. Principal-component analysis (PCA) plots of sample-to-sample distances of NK cells expanded with K562-mIL-21 or 221-mIL-21 cells show a significant difference at day 7, compared with expanded NK cells at day 14 (Figure 6A). Therefore, the following RNA-seq data analysis was mainly focused on data at day 7. Expectedly, the numbers of differentially expressed genes (DEGs) in NK cells that were expanded with 221-mIL-21 feeder cells compared to K562-mIL-21 feeder cells on day 7 by mean average (MA) plots were significantly increased, compared with the number of DEGs on day 14 (Figures 6B and 6C). Interestingly, gene set enrichment analysis (GSEA) using Gene Ontology biological process (GO_BP) datasets and hallmark datasets in the Molecular Signatures Database (MSigDB) showed that gene signatures associated with cellular amino acid metabolic process and glycolysis were upregulated in NK cells that were expanded with the 221-mIL-21 feeder cell expansion system on day 7, compared to NK cells expanded with the K562-mIL-21 feeder cell expansion system, which has been further verified by glucose uptake assays (Figures 6D–6G; Figures S11A–S11C, S12A, and S12B).

Unexpectedly, gene signatures of lymphocyte activation, lymphocyte differentiation, and cell-cell adhesion in NK cells expanded with the 221-mIL-21 feeder cell expansion system on day 7 were significantly downregulated, compared to NK cells expanded with the K562-mIL-21 feeder cell expansion system (Figures 6H–6J; Figures S11A, and S11D–S11F), which can be further illustrated by heatmaps of NK cell development and maturation, inhibitory receptors, activating receptors, and cytotoxic function (Figures 6K–6N; Figures S12C–12E).

In vitro incubation of cytokines IL-12, IL-15, and IL-18 can generate antigen-nonspecific, cytokine-induced, memory-like NK cells.[50–53] Several genes are related to these "adaptive NK cells" that are linked to reduced expression of several transcription factors and signaling proteins.[54,55] Thus, we generated a heatmap of memory-like NK-cell-related genes (Figure S13). Specifically, *PLZF* (pro-AML zinc finger) and *FCER1G* (FcR-γ) genes from 221-mIL-21 expanded NK

Figure 5. Superior Anti-tumor Activity from 221-mIL-21 Expanded CD19-CAR-NK Cells in Lymphoma Xenograft Models

(A) Diagram of the experimental design of the Raji lymphoma xenograft model. Male (n = 5) and female (n = 5) NSG mice were injected i.v. with 2×10^6 Raji-FFLuc-GFP cells in 100 μL PBS via tail vein on day 0. On day 2 and day 4, mice were injected i.v. with 1×10^7 K562-mIL-21 expanded CD19-CAR-NK cells and 221-mIL-21 expanded CD19-CAR-NK cells, respectively, in 100 μL PBS and injected i.p. with IL-2 (50,000 U per mouse) and IL-15 (10 ng per mouse) in 150 μL PBS. Animals were imaged using the IVIS system once a week for tumor growth evaluation. (B) Representative images of tumor burden at indicated time points in male mice. The range of fluorescence intensity is from 5×10^5 to 1×10^7 U of photons/s/cm^2/sr for day 7 and from 2×10^7 to 5×10^8 U of photons/s/cm^2/sr for day 14 and day 21. (C) Representative images of tumor burden at indicated time points in female mice. The range of fluorescence intensity is from 2×10^5 to 5×10^6 U of photons/s/cm^2/sr for day 7 and from 2×10^7 to 5×10^8 U of photons/s/cm^2/sr for day 14 and day 21. (D) Kaplan-Meier survival curves of tumor-bearing mice after treatment with PBS, K562-mIL-21 expanded-CD19-CAR-NK cells, and 221-mIL-21 expanded-CD19-CAR-NK cells. The p value was analyzed by log-rank (Mantel-Cox) test. (E) Quantitative data of tumor burden at indicated time points. Mice were imaged at the indicated days to evaluate tumor burden expressed as quantified, which represents tumor growth. (F) Quantitative data of mice body weight at the indicated days. (G) Diagram of the experimental design of the Daudi lymphoma xenograft model. Male (n = 2) and female (n = 3) NSG mice (n = 5 in total) were injected i.v. with 2×10^6 Daudi-FFLuc cells in 100 μL PBS via tail vein on day −4. Beginning on day 0, mice were injected i.v. with 1×10^7 221-mIL-21 expanded or K562-mIL-21 expanded CD19-CAR-NK cells in 100 μL PBS and injected i.p. with IL-2 (50,000 U per mouse) and IL-15 (10 ng per mouse) in 150 μL PBS at days 0, 3, 7, and 10. Animals were imaged using the IVIS system twice a week for tumor cell tracking. (H) Representative images of tumor burden at indicated time points. The range of fluorescence intensity is from 1×10^5 to 2×10^6 U of photons/s/cm^2/sr. (I) Quantitative data of tumor burden at indicated time points. Mice were imaged at the indicated days to evaluate tumor burden expressed as quantified bioluminescence (average light intensity), which represents tumor growth. (J) Quantitative data of mice body weight at the indicated days. ns (no significant differences) indicate $p > 0.05$. Error bars represent SEM.

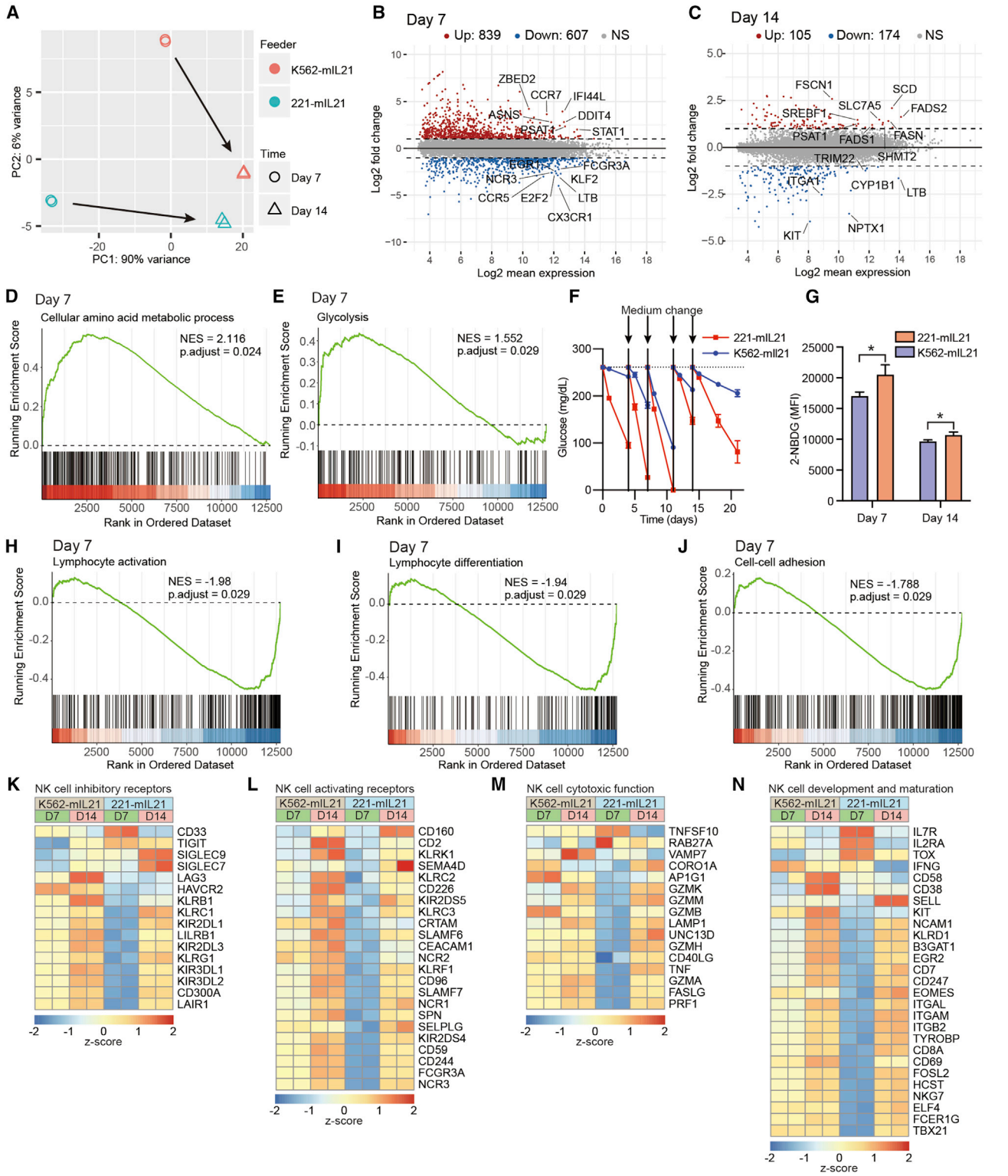

Figure 6. 221-mIL-21 Expanded NK Cells Show Enriched Metabolic Pathways and Less Differentiated Phenotypes

(A) PBMCs were stimulated with irradiated K562-mIL-21 and 221-mIL-21 feeder cells. NK cells were purified from expanded cells using flow cytometry on day 7 and day 14 for RNA-seq. Principal-component analysis (PCA) plots of sample-to-sample distances of NK cells expanded with K562-mIL21 or 221-mIL-21 feeder cells on day 7 and day

(legend continued on next page)

cells at day 7 were downregulated, compared to NK cells expanded with the K562-mIL-21 feeder cell expansion system, which indicates the enhancement of memory-like NK-cell-related genes in 221-mIL-21 expanded NK cells.

Previous studies show that cytokines (e.g., IL-2) can promote Fas (also known as CD95) and Fas-ligand (Fas-L, also known as CD95L or CD178) expression in human NK cells.[56] We compared the *FAS* and *FASL* genes from 221-mIL-21 expanded NK cells and K562-mIL-21 expanded NK cells. 221-mIL-21 expanded NK cells showed lower levels of FAS gene expression at the late expansion phase (at day-14 expansion), and *FASL* gene expression at the early expansion phase (at day-7 expansion), compared to NK cells expanded with the K562-mIL-21 feeder cell expansion system (Figure S14). These data suggest that limited fratricide events on the 221-mIL-21 feeder cell expansion system occurred, compared to NK cells expanded with the K562-mIL-21 feeder cell expansion system.

Previous studies show that mIL-21 expression on feeder cells increases the telomere length in NK cells, which may provide one underlying mechanism for sustained NK proliferation.[41] There are several genes that are significantly implicated in telomere length regulation,[57] which include *ZNF257*, *TERT*, *LRRC34*, and *NAF1* genes. Comparison analysis of positive telomere length regulator genes between 221-mIL-21 expanded NK cells and K562-mIL-21 expanded NK cells using RNA-seq data showed that *ZNF257*, *TERT*, *LRRC34*, and *NAF1* genes significantly were upregulated in 221-mIL-21 expanded NK cells, compared to K562-mIL-21 expanded NK cells (Figure S15). Thus, the data indicate that 221-mIL-21 feeder cells might regulate the telomere length of NK cells.

In conclusion, the 221-mIL-21 feeder cell expansion system promotes not only a less differentiated and more memory-like NK cell development but also fewer fratricide events among expanded NK cells. This may relate to the enriched metabolic pathways in 221-mIL-21 expanded NK cells.

Verification of the Altered Gene Expression by Quantitative RT-PCR (qRT-PCR)

To verify the changes in gene expression in the NK cells expanded by 221-mIL-21 and K562-mIL-21 using RNA-seq, we performed qRT-PCR of genes selected on the basis of their roles in the amino acid and glucose/NAD (nicotinamide adenine dinucleotide) metabolic pathways that have been discovered in the RNA-seq datasets. Normalized RNA expression relative to *ACTB* (human β-actin) was used to calculate the fold changes of 9 genes in the 221-mIL-21 expanded NK cells versus K562-mIL-21 expanded NK cells using RNA from sorted NK cells (Figure S16). Among the genes evaluated, we classified these genes into three main groups. The amino acid metabolic pathways (e.g., *MYC* [basic-helix-loop-helix, or bHLH, transcription factor], *SLC7A5* [large neutral amino acids transporter small subunit 1], *TFRC* [transferrin receptor], *CBS* [serine sulfhydrase], *PSPH* [phosphoserine phosphatase], *PSAT1* [phosphoserine aminotransferase 1], and *CTH* [cystathionine gamma-lyase]) and the glucose/NAD metabolic pathway (e.g., *MDH1* [malate dehydrogenase 1] and *PDHA1* [pyruvate dehydrogenase E1 subunit alpha 1]) were confirmed to be increased in expression in 221-mIL-21 expanded NK cells (Figure S16), which is consistent with the results from RNA-seq data. In summary, the qRT-PCR data confirm the enriched metabolic pathways in 221-mIL-21 expanded NK cells.

DISCUSSION

Recent clinical trials testing cancer immunotherapies have shown promising results for treating various cancers. Due to the recent bloom of NK-cell-mediated immunotherapies, rapid NK cell expansion techniques from various allogeneic sources are urgently needed.[9] Recent studies have shown that using 4-1BBL (4-1BBL/CD137L) and IL-21-expressing K562 cells as feeder cells can be used to rapidly expand NK cells *in vitro*.[41]

14. (B) Mean average (MA) plots of differentially expressed genes (DEGs) in NK cells expanded with 221-mIL-21 feeder cells compared to those that were expanded with K562-mIL-21 feeder cells on day 7; p values were calculated using DESeq2. Top 15 significant DEGs are labeled on the MA plot. Up, upregulated DEGs, adjusted $p < 0.05$, and $\log_2$ fold change ≥ 1; Down, downregulated DEGs, adjusted $p < 0.05$, and $\log_2$ fold change ≤ -1; NS, not significant. (C) MA plots of DEGs in NK cells that were expanded with 221-mIL-21 feeder cells compared to those that were expanded with K562-mIL-21 feeder cells on day 14. Top 15 significant DEGs are labeled on the MA plot. Up, upregulated DEGs, adjusted $p < 0.05$, and $\log_2$ fold change ≥ 1; Down, downregulated DEGs, adjusted $p < 0.05$, and $\log_2$ fold change ≤ -1; NS, not significant. (D) Gene set enrichment analysis (GSEA) of cellular amino acid metabolic processes in NK cells that were expanded with 221-mIL-21 feeder cells compared to those that were expanded with K562-mIL-21 feeder cells on day 7 using Gene Ontology biological process (GO_BP) datasets in the Molecular Signatures Database (MSigDB). NES, normalized enrichment score; p.adjust, false discovery rate (FDR)-adjusted p value. (E) GSEA of glycolysis in NK cells that were expanded with 221-mIL-21 feeder cells compared to those that were expanded with K562-mIL-21 feeder cells on day 7 using Hallmark datasets in the MSigDB. NES, normalized enrichment score; p.adjust, FDR-adjusted p value. (F) Dynamic level of glucose in the media during NK cell expansion using K562-mIL-21 and 221-mIL-21 as feeder cells. Arrows indicate the time points for media change. (G) Quantitative glucose uptake comparison of NK cells expanded with K562-mIL-21 or with 221-mIL-21 feeder cells on day 7 and day 14. *$p < 0.05$. Error bars represent SEM. (H) GSEA of lymphocyte activation in NK cells that were expanded with 221-mIL-21 feeder cells compared to those that were expanded with K562-mIL-21 feeder cells on day 7 using GO_BP datasets in the MSigDB. NES, normalized enrichment score; p.adjust, FDR-adjusted p value. (I) GSEA of lymphocyte differentiation in NK cells that were expanded with 221-mIL-21 feeder cells compared to those that were expanded with K562-mIL-21 feeder cells on day 7 using GO_BP datasets in the MSigDB. NES, normalized enrichment score; p.adjust, FDR-adjusted p value. (J) GSEA of cell-cell adhesion in NK cells that were expanded with 221-mIL-21 feeder cells compared to those that were expanded with K562-mIL-21 feeder cells on day 7 using GO_BP datasets in the MSigDB. NES, normalized enrichment score; p.adjust, FDR-adjusted p value. (K) Heatmap of inhibitory receptor of NK cells. (L) Heatmap of activating receptor of NK cells. (M) Heatmap of genes associated with cytotoxic function of NK cells. (N) Heatmap of genes associated with development and maturation of NK cells. Heatmaps were generated using *Z* scores derived from transformed RNA-seq counts using regularized-logarithm transformation (rlog). Each column represents a biological replicate.

In this study, we compared the K562-mIL-21 feeder cell expansion system with the 221-mIL-21 feeder cell expansion system to propagate human PBNK, CBNK, and CAR-NK cells. We demonstrated the superiority of the 221-mIL-21 feeder cell expansion system and presented a possible biological explanation that suggests that our feeder cell expansion system promotes a less differentiated, memory-like NK cell development, with enriched metabolic pathways and fewer fratricides.

The characterization and application of these NK cells for the treatment of patients is essential to ensure that the cells are functional and healthy. In addition, specific CAR-NK cell expansion is also needed to advance NK cell immunotherapy *in vivo*. One potential issue with NK cell expansion *in vitro* using irradiated feeder cells in the presence of cytokine IL-2 is that naive immune cells become exhausted or senescent after rapid proliferation and differentiation.[58] Indeed, CAR-modified immune cells do express exhaustion markers such as PD-1.[59–62] To solve the problem of immune cell exhaustion, one approach is to block PD-1 signaling in CAR-modified T cells.[60] Another potential strategy is to alter the metabolic pathway in CAR-modified T cells[63] or reinforce lymphocyte metabolism,[64] given the existence of essential metabolic signaling in T cells.[65] The 221 feeder cell expansion system shows that alteration of metabolic pathways can enhance NK cell expansion and result in reduced exhaustion, which is consistent with this concept in CAR-T cells.

Currently, the expansion of CAR-modified T and NK cells requires *in vitro* stimulation of genetically modified T and NK cells using antibodies and cytokines. Antibody- and cytokine-driven activation and expansion may negatively alter CAR-T or CAR-NK cell functions. For example, CAR-modified immune cell exhaustion can be induced by the end of an extensive expansion program, which is evident by the marked upregulation of PD-1, TIM-3, and LAG-3 in CAR-T cells.[66] Therefore, new expansion strategies that do not facilitate exhaustion must be developed *in vivo*, given that immune cell exhaustion is a major contributor to compromised antitumor and antiviral immune responses following chronic antigen stimulation.[67,68] Additionally, the current expansion methodology of CAR-modified immune cells for clinical applications takes at least 2 to 3 weeks, which becomes a significant hurdle for some patients. The "sleeping beauty transposon," or piggyBac system, which is capable of delivering large (9.1 to 14.3-kb) transposable elements without a significant reduction in T cell efficacy,[69–71] in combination with genetically engineered artificial cells expressing membrane-bound IL-15 and 4-1BBL, has already been used for CAR-T cell immunotherapy. This approach may promise the rapid expansion of NK cells in the future.

Currently, the K562-mIL-21 or K562-mIL-15 system is widely used in the field of NK and CAR-NK adoptive therapy.[72–74] Compared to NK expansion systems developed by other groups,[41,75] the 221 NK expansion system possesses several distinct advantages. First, the number of expanded NK cells is significantly higher in our system (an average 39,663-fold increase in 221-mIL-21 versus an average 3,588-fold increase in K562-mIL-21) due to the novel combination of the membrane form of IL-21 with two soluble cytokines in cell culture, which efficiently propagated NK cells *in vitro*. In this study, we did not compare side-by-side the other K562-mIL-21 cell lines generated by different investigators. Different expansion capability and function of NK cells using different feeder cell lines can be expected. These differences in proliferation and function could be the variants between cell-line-to-cell-line and lab-to-lab differences. Second, the 221-mIL-21 NK system shows higher purities of NK cells while enhancing cytotoxicity, compared to those from the K562-mIL-21 NK system. Third, we developed a novel approach to generate CAR-NK cells derived from CB using the 221-mIL-21 NK expansion platform. CB-derived CAR-NK cells have distinct advantages, as they are available from CB banks, and CB-derived CAR-NK cells can be used as an "off-the-shelf" CAR product. Finally, we interrogated the possible mechanism of the superiority of the 221 feeder cell expansion system by phenotyping and performing RNA-seq assays on both expanded NK cells and feeder cells. In this study, we not only provide side-by-side *in vivo* animal data but also explore the potential underlying mechanism research using RNA-seq with verification.

The RNA-seq data provided in this study will pave the way for other studies seeking to optimize NK cells or CAR-NK cells by enhancing NK cell metabolic activity. We propose that the superiority of the 221 feeder cell expansion system can be related to the capability of this system to promote a less differentiated, limited fratricidal, memory-like NK cell development.

The possible mechanisms of the superiority of the 221 feeder cell expansion system can be proposed as follows:

(1) Difference on the HLA gene expression patterns between 221-mIL-21 and K562-mIL-21 feeder cells. NK cells can interact with these MHC molecules on feeder cells via their inhibitory receptors. These inhibitory receptors can result in the "licensing" of NK cells,[76,77] which endows NK cells with superior expansion and responsiveness to subsequent activation via an immunoreceptor tyrosine-based inhibition motif (ITIM)-dependent manner, as NK cells in the absence of interaction between HLA molecules and inhibitory receptors remain unlicensed and hyporesponsive.[78] Meanwhile, the extremely low level of HLA molecule expression on 221 cells may prevent the activation-induced NK cell death that is evidenced by the low CD69 expression on NK cells expanded by 221-mIL-21 feeder cells.
(2) Enhanced expression of co-stimulatory molecules on 221-mIL-21 feeder cells, such as 4-1BBL and OX40L. Indeed, 221-mIL-21 feeder cells show greater surface expression levels of 4-1BBL molecules compared to K562-mIL-21 feeder cells in this NK expansion system, which may contribute to enhanced NK cell expansion using the 221-mIL-21 feeder cell system.
(3) The Epstein-Barr virus (EBV) transformation status on 221-mIL-21 feeder cells. Both 221 and K562 cells are frequently used to evaluate NK cell function in the field of NK cell research, because both cell lines are considered as HLA null cell lines. However, the different HLA-I/II expression levels between 221 and K562 cells

demonstrated in this study indicates that they express different HLA ligands for inhibitory receptors, which affects NK cell expansion and activation. EBV-transformed lymphoblastoid B cell lines have been used for the activation and proliferation of NK cells.[79] A previous study shows that NK cells activated by EBV-positive B cells have a specific phonotype that can overcome apoptotic mechanisms of drug resistance in hematological cancer cells.[80] Particularly, EBV infection status on 221-mIL-21 feeder cells with different HLA-I/II expression can optimize NK cell expansion, which is consistent with previous studies showing optimal NK cell activation with 221 and EBV$^+$ lymphoblastoid cells.[80–83]

(4) Induction of memory-like NK cell generation with several enriched metabolic pathways. The correlation between the superiority of 221 feeder cell expansion and the enriched metabolic pathways is clear in the RNA-seq data in this study. Long-lasting memory-like NK cells play important roles in infection, inflammation, and cancer.[84] The exact molecular mechanisms underlying the memory-like NK cell generation with 221-mIL-21 feeder cells need to be investigated further.

(5) Limited fratricidal events on 221-mIL-21 expanded NK cells. In addition to superior proliferation capability promoted by the 221-mIL-21 feeder cell expansion system, limited fratricidal events can also contribute to the 221-mIL-21 expanded NK cell number and function. Fas- and FasL-mediated fratricidal cell death is a common phenomenon in activated T and NK cells.[85,86] The lower percentage of apoptotic 221-mIL-21 expanded NK cells support the hypothesis of limited, less extensive fratricidal events on 221-mIL-21 expanded NK cells.

In conclusion, we have developed a novel platform using a 221-mIL-21 expansion system to generate primary NK and CAR-NK cells from both peripheral blood and CB. Total NK number and purity as well as functionality of these expanded NK cells are superior to those expanded using the existing K562-mIL-21 expansion system. Thus, this expansion platform will greatly support clinical use of NK immunotherapy.

MATERIALS AND METHODS

Antibodies and Reagents

Phycoerythrin (PE) and Allophycocyanin (APC) anti-human CD3 antibody (clone OKT3); fluorescein isothiocyanate (FITC); BV605, PE/Cy7, and BV 510 anti-human CD56 antibody (clone HCD56); PE anti-human CD69 antibody (clone FN50); PE/Cy7 anti-human CD8a antibody (clone HIT8a); AF647 anti-human IL-21 antibody (clone 3A3-N2); APC/Fire 750 anti-human CD226 antibody (DNAM-1) (clone 11A8); APC/Fire 750 anti-human KLRG1 (MAFA) antibody (clone SA231A2); BV 421 anti-human CD335 (NKp46) antibody (clone 9E2); PE/Cy7 anti-human CD158b (KIR2DL2/L3) antibody (clone DX27); PE/Cy7 anti-human CD244 (2B4) antibody (clone C1.7); PE anti-human CD152 (CTLA-4) antibody (clone BNI3); APC anti-human CD366 (Tim-3) antibody (clone F38-2E2); PerCP/Cy5.5 anti-human TIGIT (VSTM3) antibody (clone A15153G); FITC anti-human CD223 (LAG-3) antibody (clone 11C3C65); and PerCP/Cy5.5 anti-human CD94 (clone DX22) were purchased from BioLegend (San Diego, CA, USA). APC anti-human CD16 antibody (clone B73.1), FITC anti-human CD3 antibody (clone UCHT1), BV480 anti-human CD85j antibody (LIR-1) antibody (clone GHI/75), BV711 anti-human CD314 (NKG2D) antibody (clone 1D11), and FITC anti-human CD107a antibody (clone H4A3) were purchased from BD Biosciences (San Jose, CA, USA). FITC anti-human KIR/CD158 antibody (clone 180704), PE anti-human KIR2DL1/KIR2DS5 antibody (clone 143211), APC anti-human KIR3DL1 antibody (clone DX9), AF405 anti-human KIR3DL2/CD158k antibody (clone 539304), APC anti-human NKG2A/CD159a antibody (clone 131411), and PE anti-human NKG2C/CD159c antibody (clone 134591) were purchased from R&D Systems. AF647 Goat anti-human IgG(H+L) F(ab')$_2$ fragment antibody was purchased from Jackson ImmunoResearch (West Grove, PA, USA).

Cell Lines

The 221 cell line was a gift from Dr. Eric O. Long (National Institute of Allergy and Infectious Diseases, National Institutes of Health). 293T, K562, and Daudi cell lines were purchased from the American Type Culture Collection (ATCC). To establish K562-mIL-21 and 721.221-mIL-21 cells, K562 and 721.221 cells were transduced with IL-21 retrovirus, respectively, and then mIL-21-positive cells were sorted using the BD FACSAria II cell sorter (BD Biosciences) using AF647 mouse IgG1 anti-human IL-21 (clone 3A3-N2). To establish the Daudi-FFLuc cell, CD19-positive Daudi cells were transduced with the lentiviral vector encoding FFLuc, as previously described.[87] K562, 221, K562-mIL-21, 221-mIL-21, Daudi, and Daudi-FFLuc cells were cultured in RPMI 1640 (Corning) supplemented with 10% (v/v) fetal bovine serum (FBS) and 100 U/mL penicillin-streptomycin (Corning) at 37°C under 5% (v/v) CO_2. For NK cell expansion, K562, 221, K562-mIL-21, and 721.221-mIL-21 cells were irradiated at a dose of 10,000 rad, washed with PBS, and then used as feeder cells. 293T was cultured in DMEM (Corning) supplemented with 10% (v/v) FBS and 100 U/mL penicillin-streptomycin (Corning) at 37°C under 5% (v/v) CO_2.

Primary NK Cell Expansion

PBMCs were isolated from buffy coats (Gulf Coast Regional Blood Center and New York Blood Center) using Lymphocyte Separation Medium (Corning). Human blood related work has been approved by the Rutgers University Institutional Review Board (IRB). For NK cell expansion, 5×10^6 PBMCs were cultured with 1×10^7 10,000-rad-irradiated feeder cells in 35 mL RPMI 1640 media with 10% FBS (Corning), 2 mM L-glutamine (Corning), 100 U/mL penicillin-streptomycin (Corning), 200 U/mL IL-2 (PeproTech), and 5 ng/mL IL-15 (PeproTech) in G-Rex 6 Multi-well cell culture plates (Wilson Wolf). Media were changed every 3–4 days, and 2×10^7 cells were kept in each well for continued culture at each time. Total cell numbers were counted using trypan blue with an automated cell counter (Nexcelom Bioscience, Lawrence, MA, USA). To determine the percentage of NK cells, cells were stained for CD3 and CD56, followed by flow cytometry analysis.

Transduction of Expanded NK Cells with CD19-CAR

To produce CD19-CAR retrovirus, 293T cells were transfected with a combination of plasmids containing CD19-CAR in SFG backbone, RDF, and PegPam3, as previously described.[87] NK cells were harvested on day 7 of expansion and transduced with CD19-CAR retrovirus in plates coated with RetroNection (Clontech). Two days later, cells were transferred to a G-Rex 6 multi-well cell culture plate and maintained in 35 mL complete RPMI 1640 media with 200 U/mL IL-2 (PeproTech) and 5 ng/mL IL-15 (PeproTech). Media were changed every 3–4 days, and 2×10^7 cells were kept in each well for continued culture at each time. Total cell numbers were counted using trypan blue with an automated cell counter (Nexcelom Bioscience, Lawrence, MA, USA). To determine the percentage of NK cells and expression of CAR, cells were stained for CD3, CD56, and anti-human IgG(H+L) $F(ab')_2$ fragment and analyzed by flow cytometry.

Flow Cytometry Analysis

PBMCs and expanded NK cells were stained with fluorescence-conjugated antibodies in FACS staining buffer (PBS with 1% FBS) on ice for 30 min, washed with PBS, and analyzed on a BD FACS LSRII or an BD LSRFortessa flow cytometer (BD Biosciences). Photomultiplier tubes (PMT) voltages were adjusted, and compensation values were calculated before data collection. Data were acquired using BD FACSDiva software (BD Biosciences) and analyzed using FlowJo software (BD Biosciences).

Flow Cytometry-Based NK Cytotoxicity Assays

K562 and 221 cells were used as target cells to determine NK cell cytotoxicity. Target cells were harvested and stained with 5 μM CellTrace CFSE (Invitrogen) in PBS for 20 min. The staining was stopped by adding complete RPMI 1640 media and then washed using PBS twice. Expanded NK cells were harvested and cocultured with 2×10^5 CFSE-labeled target cells at 5 different E (effector cell) :T (target cell) ratios (4:1, 2:1, 1:1, 0.5:1, and 0.25:1, respectively) in V-bottomed 96-well plates in complete RPMI 1640 media. After 4 h of incubation at 37°C in the presence of 5% CO_2, cells were stained with 7-AAD (eBioscience) and then analyzed by flow cytometry. Target cells ($CFSE^+$) were gated, and the percentage of $7\text{-}AAD^+$ cells was used to calculate NK cell cytotoxicity using the following equation: (experimental − spontaneous dead cells)/(100 − spontaneous dead cells) × 100%.

CD107a Degranulation Assay

The CD107a degranulation assay was described previously.[88] Briefly, expanded NK cells (5×10^4) were incubated with 1.5×10^5 K562 cells in V-bottomed 96-well plates in complete RPMI 1640 media at 37°C for 2 h. The cells were harvested; washed; stained for CD3, CD56, and CD107a with GolgiStop for 30 min; and analyzed by flow cytometry.

RNA Isolation and qRT-PCR

NK cells were expanded for 7 days, sorted for $CD3^-CD56^+$ by flow cytometry, and lysed in 1.0 mL TRIzol (Thermo Fisher Scientific). After RNA isolation, RNA were checked to determine the purity and concentration by a spectrophotometer. For cDNA preparation, RNA was reverse-transcribed into cDNA using oligo(dT) cDNA Synthesis Kits (Thermo Fisher Scientific). All primers were custom synthesized and purchased from GeneWiz (South Plainfield, NJ, USA) or Integrated DNA Technologies (IDT; Newark, NJ, USA). All primers used are listed in Figure S16. qPCR reactions were performed using Quantstudio 3 (Thermo Fisher Scientific) with RT^2 SYBR Green qPCR Mastermix (QIAGEN). Differences in gene expression were normalized to *ACTB* and calculated using the $2^{-\Delta\Delta Ct}$ method according to the manufacturer's instructions.

CFSE Proliferation Assay

To compare the proliferation of 221-mIL-21 and K562-mIL-21, we used a standard CFSE proliferation assay.[89] Briefly, PBMCs were labeled with 5 μM CFSE (Thermo Fisher Scientific) in PBS and incubated at 37°C for 20 min. Then, labeled cells were quenched with RPMI containing 10% FBS and washed. Cells were then put into culture with either K562-mIL-21 or 221-mIL-21 feeder cells in a 2:1 ratio. Cultures were supplemented with IL-2 and IL-15 as described earlier. At expansion days 4, NK cells were collected, counted, and detected by flow cytometry after staining with CD3 and CD56 using a BD LSRFortessa X-20 analyzer (BD Biosciences, San Jose, CA, USA). CFSE labeling on gated NK cells was analyzed with proliferation modeling using FlowJo Software (BD Biosciences).

Annexin V Apoptosis Assay

To compare the apoptosis of 221-mIL-21-expanded NK cells and K562-mIL-21-expanded NK cells, we used an Annexin V apoptosis assay.[90] Apoptotic NK cells were stained using FITC Annexin V Apoptosis Detection Kit I (BD Biosciences, San Jose, CA, USA) per the manufacturer's instructions. The labeled NK cells were analyzed by flow cytometry. Briefly, NK cells were stimulated with feeder cells in the presence of IL-2 and IL-15, as described earlier. Flow cytometry analysis was conducted on days 3 and 8 during NK cell expansion. Cells were collected and stained for CD3 and CD56 for NK gating. Then, cells were washed with PBS and resuspended in 1× Annexin-V FLUOS binding buffer at a concentration of 10^6 NK cells per microliter. Then, cells were incubated with Annexin V-FITC and propidium iodide (PI) for 15 min, washed, and analyzed by flow cytometry using a BD LSRFortessa X-20 analyzer (BD Biosciences, San Jose, CA, USA). Approximately 10,000 events were collected per sample and analyzed by FlowJo Software (BD Biosciences).

Animal Studies

All animal experiments were approved by the Rutgers University Institutional Animal Care and Use Committee (IACUC). NSG mice from Jackson Laboratory were used for all *in vivo* experiments. To establish a human lymphoma xenograft model, both male and female NSG mice (8 weeks old) were intravenously (i.v.) injected with 2×10^6 FFLuc-Daudi cells or FFLuc-Raji cells in 100 μL PBS via tail vein at day −4. Beginning on day 0, the mice were injected i.v. with 1×10^7 221-mIL-21 expanded or K562-mIL-21 expanded CD19-CAR-NK cells in 100 μL PBS and then

injected intraperitoneally (i.p.) with IL-2 (50,000 U per mouse) and IL-15 (10 ng per mouse) in 150 μL PBS at days 0, 3, 7, and 10. Isoflurane-anesthetized animals were imaged using the IVIS system (IVIS-200, PerkinElmer, Waltham, MA, USA) 10 min after 150 mg/kg D-luciferin (Gold Biotechnology, St. Louis, MO, USA) per mouse was administered i.p. The photons emitted from the luciferase-expressing tumor cells were quantified using Living Image software v.64 (Caliper Life Sciences, Hopkinton, MA, USA). A pseudo-color image representing light intensity (blue signifying least intense and red signifying most intense) was generated and superimposed over the grayscale reference image. A constant region of interest (ROI) was drawn over the whole animal, excluding the tail, and the intensity of the signal was measured as total photons per second. After effector CD19-CAR-NK cell injections, animals were imaged twice a week for tumor cell tracking at the preclinical imaging core of the Houston Methodist Research Institute.

RNA-Seq Sample Preparation, Sequencing, and Data Analysis

NK cells were expanded among PBMCs with irradiated 221-mIL-21 and K562-mIL-21 cells as described earlier. On day 7 and day 14 of expansion, cells were collected and stained with PE-anti-CD3 and PE/Cy7-anti-CD56 antibodies on ice for 30 min. After washing with FACS staining buffer (PBS with 2% FBS) twice, cells were resuspended in FACS staining buffer, and then $CD3^-$ $CD56^+$ cells were sorted to a purity of >98% for each replicate using the BD FACSAria II cell sorter (BD Biosciences). Purified NK cells were directly lysed in TRIzol Reagent (Thermo Fisher Scientific) for RNA extraction using the manufacturer's protocol. RNA-seq was performed on a BGISEQ-500 platform by the BGI Group (Shenzhen, Guangdong, China). Clean reads in FASTQ format were obtained after filtering low-quality reads (reads where more than 50% of the base's qualities are lower than 15), reads with adaptors, and reads with more than 10% unknown bases (N). FASTQ files were aligned to the hg38 human reference genome using STAR v.2.6.1d. The aligned files were processed using the GenomicAlignments package (v.1.20.0) to get count matrices. Genes with a median of fewer than 10 reads were pre-filtered in all comparisons as an initial step. DEGs were identified using the DESeq2 package (v.1.24.0) and were defined as having an adjusted $p < 0.05$ and a $\log_2$ fold change ≥ 1 or ≤ -1. The $\log_2$ fold changes were shrunken using the lfcShrink function and were then used to make MA plots using the ggpubr package (v.0.2.1). GSEAs were performed using MSigDB (Broad Institute) and the clusterProfiler package (v.3.12.0). Heatmaps were generated using Z scores derived from log-transformed counts. All of the data analysis was performed using R (v.3.6.0).

Statistical Analysis

Data were represented as means ± SEM or means ± SD (the standard error of the mean). The statistical significance was determined using a two-tailed unpaired Student t test, a two-tailed paired Student t test, and a two-way ANOVA, where indicated. $p < 0.05$ was considered statistically significant.

SUPPLEMENTAL INFORMATION

Supplemental Information can be found online at https://doi.org/10.1016/j.omtm.2020.06.014.

AUTHOR CONTRIBUTIONS

Y.Y., S.B., and D.L. designed the study and wrote the manuscript. M.M., H.-C.T., T.L., J.-G.J., and C.L. assisted with experiments. D.L. conceived and supervised the study.

CONFLICTS OF INTEREST

The authors declare no competing interests.

ACKNOWLEDGMENTS

We would like to thank the members of the Liu laboratory for their comments on the manuscript. We also would like to thank Dr. Eric Long (National Institute of Allergy and Infectious Diseases [NIAID]/NIH) for the 721.221 cell line and Dr. Gianpietro Dotti (UNC) for the SFG vectors. This work was supported in part by National Heart, Lung, and Blood Institute grant HL125018 and NIAID grants AI124769, AI129594, and AI130197 (all to D.L.); a Houston Methodist Career Cornerstone award; Baylor-UT Houston Center for AIDS Research Core Support grant no. AI036211 from the NIAID; and Rutgers University–New Jersey Medical School Liu Laboratory Startup funding.

REFERENCES

1. Long, E.O., Kim, H.S., Liu, D., Peterson, M.E., and Rajagopalan, S. (2013). Controlling natural killer cell responses: integration of signals for activation and inhibition. Annu. Rev. Immunol. *31*, 227–258.
2. Rosenberg, E.B., McCoy, J.L., Green, S.S., Donnelly, F.C., Siwarski, D.F., Levine, P.H., and Herberman, R.B. (1974). Destruction of human lymphoid tissue-culture cell lines by human peripheral lymphocytes in 51Cr-release cellular cytotoxicity assays. J. Natl. Cancer Inst. *52*, 345–352.
3. Kiessling, R., Klein, E., Pross, H., and Wigzell, H. (1975). "Natural" killer cells in the mouse. II. Cytotoxic cells with specificity for mouse Moloney leukemia cells. Characteristics of the killer cell. Eur. J. Immunol. *5*, 117–121.
4. Kiessling, R., Klein, E., and Wigzell, H. (1975). "Natural" killer cells in the mouse. I. Cytotoxic cells with specificity for mouse Moloney leukemia cells. Specificity and distribution according to genotype. Eur. J. Immunol. *5*, 112–117.
5. Herberman, R.B., Nunn, M.E., Holden, H.T., and Lavrin, D.H. (1975). Natural cytotoxic reactivity of mouse lymphoid cells against syngeneic and allogeneic tumors. II. Characterization of effector cells. Int. J. Cancer *16*, 230–239.
6. Herberman, R.B., Nunn, M.E., and Lavrin, D.H. (1975). Natural cytotoxic reactivity of mouse lymphoid cells against syngeneic acid allogeneic tumors. I. Distribution of reactivity and specificity. Int. J. Cancer *16*, 216–229.
7. Liu, D., Bryceson, Y.T., Meckel, T., Vasiliver-Shamis, G., Dustin, M.L., and Long, E.O. (2009). Integrin-dependent organization and bidirectional vesicular traffic at cytotoxic immune synapses. Immunity *31*, 99–109.
8. Liu, D., Peterson, M.E., and Long, E.O. (2012). The adaptor protein Crk controls activation and inhibition of natural killer cells. Immunity *36*, 600–611.
9. Liu, D., Tian, S., Zhang, K., Xiong, W., Lubaki, N.M., Chen, Z., and Han, W. (2017). Chimeric antigen receptor (CAR)-modified natural killer cell-based immunotherapy and immunological synapse formation in cancer and HIV. Protein Cell *8*, 861–877.
10. Liu, E., Marin, D., Banerjee, P., Macapinlac, H.A., Thompson, P., Basar, R., Nassif Kerbauy, L., Overman, B., Thall, P., Kaplan, M., et al. (2020). Use of CAR-Transduced Natural Killer Cells in CD19-Positive Lymphoid Tumors. N. Engl. J. Med. *382*, 545–553.

11. Miller, J.S., Soignier, Y., Panoskaltsis-Mortari, A., McNearney, S.A., Yun, G.H., Fautsch, S.K., McKenna, D., Le, C., Defor, T.E., Burns, L.J., et al. (2005). Successful adoptive transfer and in vivo expansion of human haploidentical NK cells in patients with cancer. Blood *105*, 3051–3057.

12. Rubnitz, J.E., Inaba, H., Ribeiro, R.C., Pounds, S., Rooney, B., Bell, T., Pui, C.H., and Leung, W. (2010). NKAML: a pilot study to determine the safety and feasibility of haploidentical natural killer cell transplantation in childhood acute myeloid leukemia. J. Clin. Oncol. *28*, 955–959.

13. Yoon, S.R., Lee, Y.S., Yang, S.H., Ahn, K.H., Lee, J.H., Lee, J.H., Kim, D.Y., Kang, Y.A., Jeon, M., Seol, M., et al. (2010). Generation of donor natural killer cells from CD34(+) progenitor cells and subsequent infusion after HLA-mismatched allogeneic hematopoietic cell transplantation: a feasibility study. Bone Marrow Transplant. *45*, 1038–1046.

14. Liu, E., Tong, Y., Dotti, G., Shaim, H., Savoldo, B., Mukherjee, M., Orange, J., Wan, X., Lu, X., Reynolds, A., et al. (2018). Cord blood NK cells engineered to express IL-15 and a CD19-targeted CAR show long-term persistence and potent antitumor activity. Leukemia *32*, 520–531.

15. Liu, D., Tian, S., Zhang, K., Xiong, W., Lubaki, N.M., Chen, Z., and Han, W. (2018). Erratum to: Chimeric antigen receptor (CAR)-modified natural killer cell-based immunotherapy and immunological synapse formation in cancer and HIV. Protein Cell *9*, 902.

16. Rezvani, K., and Rouce, R.H. (2015). The Application of Natural Killer Cell Immunotherapy for the Treatment of Cancer. Front. Immunol. *6*, 578.

17. Hermanson, D.L., and Kaufman, D.S. (2015). Utilizing chimeric antigen receptors to direct natural killer cell activity. Front. Immunol. *6*, 195.

18. Glienke, W., Esser, R., Priesner, C., Suerth, J.D., Schambach, A., Wels, W.S., Grez, M., Kloess, S., Arseniev, L., and Koehl, U. (2015). Advantages and applications of CAR-expressing natural killer cells. Front. Pharmacol. *6*, 21.

19. Porter, D.L., Levine, B.L., Kalos, M., Bagg, A., and June, C.H. (2011). Chimeric antigen receptor-modified T cells in chronic lymphoid leukemia. N. Engl. J. Med. *365*, 725–733.

20. Kim, M.G., Kim, D., Suh, S.K., Park, Z., Choi, M.J., and Oh, Y.K. (2016). Current status and regulatory perspective of chimeric antigen receptor-modified T cell therapeutics. Arch. Pharm. Res. *39*, 437–452.

21. Maude, S., and Barrett, D.M. (2016). Current status of chimeric antigen receptor therapy for haematological malignancies. Br. J. Haematol. *172*, 11–22.

22. Davila, M.L., Riviere, I., Wang, X., Bartido, S., Park, J., Curran, K., Chung, S.S., Stefanski, J., Borquez-Ojeda, O., Olszewska, M., et al. (2014). Efficacy and toxicity management of 19-28z CAR T cell therapy in B cell acute lymphoblastic leukemia. Sci. Transl. Med. *6*, 224ra25.

23. Maude, S.L., Frey, N., Shaw, P.A., Aplenc, R., Barrett, D.M., Bunin, N.J., Chew, A., Gonzalez, V.E., Zheng, Z., Lacey, S.F., et al. (2014). Chimeric antigen receptor T cells for sustained remissions in leukemia. N. Engl. J. Med. *371*, 1507–1517.

24. Lee, D.W., Kochenderfer, J.N., Stetler-Stevenson, M., Cui, Y.K., Delbrook, C., Feldman, S.A., Fry, T.J., Orentas, R., Sabatino, M., Shah, N.N., et al. (2015). T cells expressing CD19 chimeric antigen receptors for acute lymphoblastic leukaemia in children and young adults: a phase 1 dose-escalation trial. Lancet *385*, 517–528.

25. Garfall, A.L., Maus, M.V., Hwang, W.T., Lacey, S.F., Mahnke, Y.D., Melenhorst, J.J., Zheng, Z., Vogl, D.T., Cohen, A.D., Weiss, B.M., et al. (2015). Chimeric Antigen Receptor T Cells against CD19 for Multiple Myeloma. N. Engl. J. Med. *373*, 1040–1047.

26. Atanackovic, D., Radhakrishnan, S.V., Bhardwaj, N., and Luetkens, T. (2016). Chimeric Antigen Receptor (CAR) therapy for multiple myeloma. Br. J. Haematol. *172*, 685–698.

27. Ahmed, N., Brawley, V.S., Hegde, M., Robertson, C., Ghazi, A., Gerken, C., Liu, E., Dakhova, O., Ashoori, A., Corder, A., et al. (2015). Human Epidermal Growth Factor Receptor 2 (HER2) -Specific Chimeric Antigen Receptor-Modified T Cells for the Immunotherapy of HER2-Positive Sarcoma. J. Clin. Oncol. *33*, 1688–1696.

28. Pule, M.A., Savoldo, B., Myers, G.D., Rossig, C., Russell, H.V., Dotti, G., Huls, M.H., Liu, E., Gee, A.P., Mei, Z., et al. (2008). Virus-specific T cells engineered to coexpress tumor-specific receptors: persistence and antitumor activity in individuals with neuroblastoma. Nat. Med. *14*, 1264–1270.

29. Louis, C.U., Savoldo, B., Dotti, G., Pule, M., Yvon, E., Myers, G.D., Rossig, C., Russell, H.V., Diouf, O., Liu, E., et al. (2011). Antitumor activity and long-term fate of chimeric antigen receptor-positive T cells in patients with neuroblastoma. Blood *118*, 6050–6056.

30. Casucci, M., Hawkins, R.E., Dotti, G., and Bondanza, A. (2015). Overcoming the toxicity hurdles of genetically targeted T cells. Cancer Immunol. Immunother. *64*, 123–130.

31. Gottschalk, S., Bollard, C.M., Straathof, K.C., Louis, C.U., Savoldo, B., Dotti, G., Brenner, M.K., Heslop, H.E., and Rooney, C.M. (2006). T cell therapies. Ernst Schering Found. Symp. Proc. (4), 69–82.

32. Ramos, C.A., Savoldo, B., and Dotti, G. (2014). CD19-CAR trials. Cancer J. *20*, 112–118.

33. Savoldo, B., and Dotti, G. (2013). Chimeric antigen receptors (CARs) from bench-to-bedside. Immunol. Lett. *155*, 40–42.

34. Bonifant, C.L., Jackson, H.J., Brentjens, R.J., and Curran, K.J. (2016). Toxicity and management in CAR T-cell therapy. Mol. Ther. Oncolytics *3*, 16011.

35. Alonso-Camino, V., Harwood, S.L., Álvarez-Méndez, A., and Alvarez-Vallina, L. (2016). Efficacy and toxicity management of CAR-T-cell immunotherapy: a matter of responsiveness control or tumour-specificity? Biochem. Soc. Trans. *44*, 406–411.

36. Kalaitsidou, M., Kueberuwa, G., Schütt, A., and Gilham, D.E. (2015). CAR T-cell therapy: toxicity and the relevance of preclinical models. Immunotherapy *7*, 487–497.

37. Gust, J., Hay, K.A., Hanafi, L.A., Li, D., Myerson, D., Gonzalez-Cuyar, L.F., Yeung, C., Liles, W.C., Wurfel, M., Lopez, J.A., et al. (2017). Endothelial Activation and Blood-Brain Barrier Disruption in Neurotoxicity after Adoptive Immunotherapy with CD19 CAR-T Cells. Cancer Discov. *7*, 1404–1419.

38. Hay, K.A., Hanafi, L.A., Li, D., Gust, J., Liles, W.C., Wurfel, M.M., López, J.A., Chen, J., Chung, D., Harju-Baker, S., et al. (2017). Kinetics and biomarkers of severe cytokine release syndrome after CD19 chimeric antigen receptor-modified T-cell therapy. Blood *130*, 2295–2306.

39. Prasad, V. (2018). Immunotherapy: Tisagenlecleucel - the first approved CAR-T-cell therapy: implications for payers and policy makers. Nat. Rev. Clin. Oncol. *15*, 11–12.

40. Shimizu, Y., Geraghty, D.E., Koller, B.H., Orr, H.T., and DeMars, R. (1988). Transfer and expression of three cloned human non-HLA-A,B,C class I major histocompatibility complex genes in mutant lymphoblastoid cells. Proc. Natl. Acad. Sci. USA *85*, 227–231.

41. Denman, C.J., Senyukov, V.V., Somanchi, S.S., Phatarpekar, P.V., Kopp, L.M., Johnson, J.L., Singh, H., Hurton, L., Maiti, S.N., Huls, M.H., et al. (2012). Membrane-bound IL-21 promotes sustained ex vivo proliferation of human natural killer cells. PLoS ONE *7*, e30264.

42. Ojo, E.O., Sharma, A.A., Liu, R., Moreton, S., Checkley-Luttge, M.A., Gupta, K., Lee, G., Lee, D.A., Otegbeye, F., Sekaly, R.P., et al. (2019). Membrane bound IL-21 based NK cell feeder cells drive robust expansion and metabolic activation of NK cells. Sci. Rep. *9*, 14916.

43. Venkatasubramanian, S., Cheekatla, S., Paidipally, P., Tripathi, D., Welch, E., Tvinnereim, A.R., Nurieva, R., and Vankayalapati, R. (2017). IL-21-dependent expansion of memory-like NK cells enhances protective immune responses against Mycobacterium tuberculosis. Mucosal Immunol. *10*, 1031–1042.

44. Ciurea, S.O., Schafer, J.R., Bassett, R., Denman, C.J., Cao, K., Willis, D., Rondon, G., Chen, J., Soebbing, D., Kaur, I., et al. (2017). Phase 1 clinical trial using mbIL21 ex vivo-expanded donor-derived NK cells after haploidentical transplantation. Blood *130*, 1857–1868.

45. Vidard, L., Dureuil, C., Baudhuin, J., Vescovi, L., Durand, L., Sierra, V., and Parmantier, E. (2019). CD137 (4-1BB) Engagement Fine-Tunes Synergistic IL-15- and IL-21-Driven NK Cell Proliferation. J. Immunol. *203*, 676–685.

46. Lozzio, B.B., and Lozzio, C.B. (1979). Properties and usefulness of the original K-562 human myelogenous leukemia cell line. Leuk. Res. *3*, 363–370.

47. Kweon, S., Phan, M.T., Chun, S., Yu, H., Kim, J., Kim, S., Lee, J., Ali, A.K., Lee, S.H., Kim, S.K., et al. (2019). Expansion of Human NK Cells Using K562 Cells Expressing OX40 Ligand and Short Exposure to IL-21. Front. Immunol. *10*, 879.

48. Nham, T., Poznanski, S.M., Fan, I.Y., Vahedi, F., Shenouda, M.M., Lee, A.J., Chew, M.V., Hogg, R.T., Lee, D.A., and Ashkar, A.A. (2018). Ex Vivo-expanded Natural Killer Cells Derived From Long-term Cryopreserved Cord Blood are Cytotoxic Against Primary Breast Cancer Cells. J. Immunother. *41*, 64–72.

49. Balassa, K., and Rocha, V. (2018). Anticancer cellular immunotherapies derived from umbilical cord blood. Expert Opin. Biol. Ther. *18*, 121–134.

50. Cooper, M.A., Elliott, J.M., Keyel, P.A., Yang, L., Carrero, J.A., and Yokoyama, W.M. (2009). Cytokine-induced memory-like natural killer cells. Proc. Natl. Acad. Sci. USA *106*, 1915–1919.

51. Keppel, M.P., Yang, L., and Cooper, M.A. (2013). Murine NK cell intrinsic cytokine-induced memory-like responses are maintained following homeostatic proliferation. J. Immunol. *190*, 4754–4762.

52. Ni, J., Miller, M., Stojanovic, A., Garbi, N., and Cerwenka, A. (2012). Sustained effector function of IL-12/15/18-preactivated NK cells against established tumors. J. Exp. Med. *209*, 2351–2365.

53. Romee, R., Schneider, S.E., Leong, J.W., Chase, J.M., Keppel, C.R., Sullivan, R.P., Cooper, M.A., and Fehniger, T.A. (2012). Cytokine activation induces human memory-like NK cells. Blood *120*, 4751–4760.

54. Lee, J., Zhang, T., Hwang, I., Kim, A., Nitschke, L., Kim, M., Scott, J.M., Kamimura, Y., Lanier, L.L., and Kim, S. (2015). Epigenetic modification and antibody-dependent expansion of memory-like NK cells in human cytomegalovirus-infected individuals. Immunity *42*, 431–442.

55. Schlums, H., Cichocki, F., Tesi, B., Theorell, J., Beziat, V., Holmes, T.D., Han, H., Chiang, S.C., Foley, B., Mattsson, K., et al. (2015). Cytomegalovirus infection drives adaptive epigenetic diversification of NK cells with altered signaling and effector function. Immunity *42*, 443–456.

56. Medvedev, A.E., Johnsen, A.C., Haux, J., Steinkjer, B., Egeberg, K., Lynch, D.H., Sundan, A., and Espevik, T. (1997). Regulation of Fas and Fas-ligand expression in NK cells by cytokines and the involvement of Fas-ligand in NK/LAK cell-mediated cytotoxicity. Cytokine *9*, 394–404.

57. Coutts, F., Palmos, A.B., Duarte, R.R.R., de Jong, S., Lewis, C.M., Dima, D., and Powell, T.R. (2019). The polygenic nature of telomere length and the anti-ageing properties of lithium. Neuropsychopharmacology *44*, 757–765.

58. Keir, M.E., Butte, M.J., Freeman, G.J., and Sharpe, A.H. (2008). PD-1 and its ligands in tolerance and immunity. Annu. Rev. Immunol. *26*, 677–704.

59. John, L.B., Kershaw, M.H., and Darcy, P.K. (2013). Blockade of PD-1 immunosuppression boosts CAR T-cell therapy. OncoImmunology *2*, e26286.

60. Cherkassky, L., Morello, A., Villena-Vargas, J., Feng, Y., Dimitrov, D.S., Jones, D.R., Sadelain, M., and Adusumilli, P.S. (2016). Human CAR T cells with cell-intrinsic PD-1 checkpoint blockade resist tumor-mediated inhibition. J. Clin. Invest. *126*, 3130–3144.

61. Chong, E.A., Melenhorst, J.J., Lacey, S.F., Ambrose, D.E., Gonzalez, V., Levine, B.L., June, C.H., and Schuster, S.J. (2017). PD-1 Blockade Modulates Chimeric Antigen Receptor (CAR) Modified T Cells and Induces Tumor Regression: Refueling the CAR. Blood *129*, 1039–1041.

62. Gargett, T., Yu, W., Dotti, G., Yvon, E.S., Christo, S.N., Hayball, J.D., Lewis, I.D., Brenner, M.K., and Brown, M.P. (2016). GD2-specific CAR T Cells Undergo Potent Activation and Deletion Following Antigen Encounter but can be Protected From Activation-induced Cell Death by PD-1 Blockade. Mol. Ther. *24*, 1135–1149.

63. Ping, Y., Liu, C., and Zhang, Y. (2018). T-cell receptor-engineered T cells for cancer treatment: current status and future directions. Protein Cell *9*, 254–266.

64. Lim, W.A., and June, C.H. (2017). The Principles of Engineering Immune Cells to Treat Cancer. Cell *168*, 724–740.

65. Buck, M.D., O'Sullivan, D., and Pearce, E.L. (2015). T cell metabolism drives immunity. J. Exp. Med. *212*, 1345–1360.

66. Long, A.H., Haso, W.M., Shern, J.F., Wanhainen, K.M., Murgai, M., Ingaramo, M., Smith, J.P., Walker, A.J., Kohler, M.E., Venkateshwara, V.R., et al. (2015). 4-1BB costimulation ameliorates T cell exhaustion induced by tonic signaling of chimeric antigen receptors. Nat. Med. *21*, 581–590.

67. Wherry, E.J. (2011). T cell exhaustion. Nat. Immunol. *12*, 492–499.

68. Virgin, H.W., Wherry, E.J., and Ahmed, R. (2009). Redefining chronic viral infection. Cell *138*, 30–50.

69. Guerrero, A.D., Moyes, J.S., and Cooper, L.J. (2014). The human application of gene therapy to re-program T-cell specificity using chimeric antigen receptors. Chin. J. Cancer *33*, 421–433.

70. Singh, H., Huls, H., Kebriaei, P., and Cooper, L.J. (2014). A new approach to gene therapy using Sleeping Beauty to genetically modify clinical-grade T cells to target CD19. Immunol. Rev. *257*, 181–190.

71. Maiti, S.N., Huls, H., Singh, H., Dawson, M., Figliola, M., Olivares, S., Rao, P., Zhao, Y.J., Multani, A., Yang, G., et al. (2013). Sleeping beauty system to redirect T-cell specificity for human applications. J. Immunother. *36*, 112–123.

72. Imai, C., Iwamoto, S., and Campana, D. (2005). Genetic modification of primary natural killer cells overcomes inhibitory signals and induces specific killing of leukemic cells. Blood *106*, 376–383.

73. Shimasaki, N., Jain, A., and Campana, D. (2020). NK cells for cancer immunotherapy. Nat. Rev. Drug Discov. *19*, 200–218.

74. Shimasaki, N., Coustan-Smith, E., Kamiya, T., and Campana, D. (2016). Expanded and armed natural killer cells for cancer treatment. Cytotherapy *18*, 1422–1434.

75. Fujisaki, H., Kakuda, H., Shimasaki, N., Imai, C., Ma, J., Lockey, T., Eldridge, P., Leung, W.H., and Campana, D. (2009). Expansion of highly cytotoxic human natural killer cells for cancer cell therapy. Cancer Res. *69*, 4010–4017.

76. Kim, S., Poursine-Laurent, J., Truscott, S.M., Lybarger, L., Song, Y.J., Yang, L., French, A.R., Sunwoo, J.B., Lemieux, S., Hansen, T.H., and Yokoyama, W.M. (2005). Licensing of natural killer cells by host major histocompatibility complex class I molecules. Nature *436*, 709–713.

77. Höglund, P., and Brodin, P. (2010). Current perspectives of natural killer cell education by MHC class I molecules. Nat. Rev. Immunol. *10*, 724–734.

78. Anfossi, N., André, P., Guia, S., Falk, C.S., Roetynck, S., Stewart, C.A., Breso, V., Frassati, C., Reviron, D., Middleton, D., et al. (2006). Human NK cell education by inhibitory receptors for MHC class I. Immunity *25*, 331–342.

79. Perussia, B., Ramoni, C., Anegon, I., Cuturi, M.C., Faust, J., and Trinchieri, G. (1987). Preferential proliferation of natural killer cells among peripheral blood mononuclear cells cocultured with B lymphoblastoid cell lines. Nat. Immun. Cell Growth Regul. *6*, 171–188.

80. Sánchez-Martínez, D., Azaceta, G., Muntasell, A., Aguiló, N., Núñez, D., Gálvez, E.M., Naval, J., Anel, A., Palomera, L., Vilches, C., et al. (2015). Human NK cells activated by EBV^+ lymphoblastoid cells overcome anti-apoptotic mechanisms of drug resistance in haematological cancer cells. OncoImmunology *4*, e991613.

81. Lisovsky, I., Isitman, G., Bruneau, J., and Bernard, N.F. (2015). Functional analysis of NK cell subsets activated by 721.221 and K562 HLA-null cells. J. Leukoc. Biol. *97*, 761–767.

82. Berg, M., Lundqvist, A., McCoy, P., Jr., Samsel, L., Fan, Y., Tawab, A., and Childs, R. (2009). Clinical-grade ex vivo-expanded human natural killer cells up-regulate activating receptors and death receptor ligands and have enhanced cytolytic activity against tumor cells. Cytotherapy *11*, 341–355.

83. Granzin, M., Stojanovic, A., Miller, M., Childs, R., Huppert, V., and Cerwenka, A. (2016). Highly efficient IL-21 and feeder cell-driven *ex vivo* expansion of human NK cells with therapeutic activity in a xenograft mouse model of melanoma. OncoImmunology *5*, e1219007.

84. Cerwenka, A., and Lanier, L.L. (2016). Natural killer cell memory in infection, inflammation and cancer. Nat. Rev. Immunol. *16*, 112–123.

85. Lynch, D.H., Ramsdell, F., and Alderson, M.R. (1995). Fas and FasL in the homeostatic regulation of immune responses. Immunol. Today *16*, 569–574.

86. Nagata, S. (1999). Fas ligand-induced apoptosis. Annu. Rev. Genet. *33*, 29–55.

87. Xiong, W., Chen, Y., Kang, X., Chen, Z., Zheng, P., Hsu, Y.H., Jang, J.H., Qin, L., Liu, H., Dotti, G., and Liu, D. (2018). Immunological Synapse Predicts Effectiveness of Chimeric Antigen Receptor Cells. Mol. Ther. *26*, 963–975.

88. Zheng, P., Noroski, L.M., Hanson, I.C., Chen, Y., Lee, M.E., Huang, Y., Zhu, M.X., Banerjee, P.P., Makedonas, G., Orange, J.S., et al. (2015). Molecular mechanisms of functional natural killer deficiency in patients with partial DiGeorge syndrome. J. Allergy Clin. Immunol. *135*, 1293–1302.

89. Muccio, L., Falco, M., Bertaina, A., Locatelli, F., Frassoni, F., Sivori, S., Moretta, L., Moretta, A., and Della Chiesa, M. (2018). Late Development of FcεRγ^{neg} Adaptive Natural Killer Cells Upon Human Cytomegalovirus Reactivation in Umbilical Cord Blood Transplantation Recipients. Front. Immunol. *9*, 1050.

90. Nabekura, T., Kanaya, M., Shibuya, A., Fu, G., Gascoigne, N.R., and Lanier, L.L. (2014). Costimulatory molecule DNAM-1 is essential for optimal differentiation of memory natural killer cells during mouse cytomegalovirus infection. Immunity *40*, 225–234.